universität wien

MASTERARBEIT / MASTER'S THESIS

Titel der Masterarbeit / Title of the Master's Thesis

^{44}Ti – AMS detection of a new Trace Isotope for Astrophysics

verfasst von / submitted by

David Krebs MSc BSc BSc

angestrebter akademischer Grad / in partial fulfilment of the requirements for the degree of

Master of Science (MSc)

Wien, 2026 / Vienna, 2026

Studienkennzahl lt. Studienblatt / degree programme code as it appears on the student record sheet:	UA 066 876
Studienrichtung lt. Studienblatt / degree programme as it appears on the student record sheet:	Masterstudium Physics
Betreut von / Supervisor:	Ass.-Prof. Dr. Karin Hain
Mitbetreut von / Co-Supervisor:	Mag. Dr. Martin Martschini

To investigate a problem is, indeed, to solve it. -毛泽东

Acknowledgements

I would like to thank everyone at the Isotope Physics Group for their contributions to my work. Without the help and very productive talks with several colleagues of the institute, none of this would have been possible. In particular, I would like to thank Martin Martschini for his supervision. His ideas, knowledge and fast response to all problems were instrumental to this thesis. I would also like to thank Karin Hain for the supervision in scientific questions, also in form of the weekly meetings. Her high standards have surely improved the quality of this work. Silke Merchel's supervision on the chemistry and cathode preparation also deserves my thanks.

I would also like to thank Zeynep Talip from the Paul Scherrer Institute for producing and sending us 12 kBq of ^{44}Ti free of charge in the spirit of scientific collaboration. Needless to say that without this sample, no ^{44}Ti could have been measured for this thesis.

Klaus Wendt, Raphael Hasse and Thorben Niemeyer from the Johannes Gutenberg-Universität Mainz shall also be thanked for their visit allowing us to test the OPO Laser for our measurements.

Among my immediate colleagues, all have contributed in some way to the final thesis through ideas, discussions and feedback. Specifically Denis Ibrahimovich, Esad Hrnjic, Laurenz Wiedermann and Stephanie Adler have always been there for discussions about methods and problems.

I would also like to thank Stephanie Adler, Laurenz Wiedermann and Alexander Wieser for proof reading and discussions on thesis writing.

My thanks also go to Vanessa Florl and Ella Woff for helping in various ways with the thesis, despite not being familiar with isotope physics.

Lastly, I want to thank my family for supporting my second masters degree with unqualified enthusiasm.

Abstract

The radioisotope ^{44}Ti, with its 58.9-year half-life, serves as a unique tracer for stellar nucleosynthesis. Detected in only two supernova remnants (Cas A and SN1987A) and some meteorites, it offers rare insights into explosion mechanisms. However, Cas A observations show $(160 \pm 60)\ \mu M_{\odot}$ of ^{44}Ti, 2–10 times higher than models predict, pointing to gaps in the understanding of core-collapse supernovae or the ^{40}Ca$(\alpha, \gamma)^{44}$Ti reaction cross sections.

Accelerator Mass Spectrometry (AMS) enables rare isotope detection through direct atom counting, but measuring ^{44}Ti is challenging due to interference from the stable isobar ^{44}Ca. Conventionally, AMS requires $\geq$6 MV accelerators for separation. The Ion-Laser InterAction Mass Spectrometry (ILIAMS) setup at the Vienna Environmental Research Accelerator (VERA) facility offers an alternative through selective isobar suppression using laser & gas interactions with ions in a gas-filled cooler. This work developed new AMS methods for detecting ^{44}Ti at VERA's 3 MV accelerator. Using 12 kBq of ^{44}Ti from PSI, in-house standards with ^{44}Ti/^{48}Ti ratios of $5 \cdot 10^{-10}$ to $5 \cdot 10^{-12}$ were prepared and measured.

Remarkable suppression was achieved through complementary mechanisms: the RFQ ion cooler via gas interaction (factor $\geq 10^6$), an OPO laser at 1325 nm (factor $\approx 10^5$), and detector separation (factor $\approx$100). Combined suppression potentially exceeds 10^{13} with full laser implementation.

The standards showed internal consistency within 40% of nominal values. The detection limit of $1.24 \cdot 10^{-13}$ is approximately 12 times higher than best literature values ($\sim 10^{-14}$ at 14 MV facilities), demonstrating VERA-ILIAMS capability for ^{44}Ti measurements while indicating room for improvement. This thesis has thus not only established a new analytical capability at VERA but has also made a tangible contribution to the tools available for exploring stellar nucleosynthesis.

Kurzfassung

Das Radioisotop ^{44}Ti mit seiner kurzen Halbwertszeit von 58,9 ± 0,3 Jahren wurde bisher nur in zwei Supernova-Überresten nachgewiesen: Cassiopeia A (Cas A) und SN1987A, sowie in einigen Meteoritenproben. Als wichtiger Indikator für stellare Nukleosynthese-Prozesse bietet ^{44}Ti einzigartige Einblicke in Supernova-Explosionen, da es nur wenige hundert Jahre nach der Explosion nachweisbar bleibt. Allerdings gibt es eine Diskrepanz zwischen Beobachtungen und theoretischen Modellen: Gamma-Messungen zeigen etwa (160±60) $\mu M_\odot$ an ^{44}Ti in Cas A, was um einen Faktor 2-10 höher ist, als von aktuellen Supernova-Nukleosynthese-Modellen vorhergesagt. Diese Diskrepanz stammt sowohl von grundlegenden Mängeln in unserem Verständnis von Kernkollaps-Supernovae und von unvollständigem Verständnis der Kernreaktionsquerschnitte, insbesondere für die primäre Produktionsreaktion ^{40}Ca(α,γ)^{44}Ti.

Accelerator Mass Spectrometry (AMS; zu deutsch Beschleuniger-Massenspektrometrie) ermöglicht den Nachweis seltener Isotope durch direktes Zählen einzelner Atome und bietet überlegene Sensitivity (dt. Empfindlichkeit) für langlebige oder sehr seltene Radionuklide. Die Messung von ^{44}Ti mittels AMS stellt jedoch eine Herausforderung dar: Das stabile Isobar ^{44}Ca, das in alltäglichen Materialien einschließlich Staub und menschlichem Schweiß häufig vorkommt, interferiert mit der Detektion. Traditionelle AMS-Anlagen benötigten hohe Beschleunigerspannungen ($\geq$6 MV), um ausreichend Energie für die Unterscheidung von ^{44}Ti und ^{44}Ca in Detektoren durch ihre unterschiedlichen Energieverlustcharakteristiken zu erreichen. Der einzigartige Ion-Laser InterAction Mass Spectrometry (ILIAMS) Aufbau am Vienna Environmental Research Accelerator (VERA) bietet einen alternativen Ansatz durch selektive Isobar-Unterdrückung. ILIAMS verwendet einen Radiofrequenz-Quadrupol (RFQ) Ionenkühler, der mit Puffergas gefüllt ist, wobei Laser-Photodetachment und kollisionsinduzierte Wechselwirkungen interferierende CaO^--Ionen unterdrücken können, während die gewünschten TiO^--Ionen weitgehend unbeeinflusst bleiben.

Diese Arbeit entwickelte neue AMS-Methoden für den Nachweis von^{44}Ti am 3 MV Tandem-Beschleuniger von VERA. Durch das Paul Scherrer Institut (PSI) wurden 12 kBq ^{44}Ti bereitgestellt und mit stabilem Ti verdünnt, um interne Standards zu erstellen. Ein einfaches chemisches Aufbereitungsverfahren wurde angewendet und TiO_2-Material mit ^{44}Ti/^{48}Ti-Verhältnissen im Bereich von $5 \cdot 10^{-10}$ bis $5 \cdot 10^{-12}$ wurde präpariert und mit AMS zusammen mit Prozess-Blanks gemessen.

Eine bemerkenswerte Unterdrückung des ^{44}Ca-Isobars wurde durch verschiedene komplementäre Mechanismen erreicht. Der RFQ-Ionenkühler lieferte eine Unterdrückung von über 10^6. Zusätzlich demonstrierte ein optisch parametrischer Oszillator (OPO) Laser bei 1325 nm eine weitere Unterdrückung von etwa 10^5. Darüber hinaus lieferte der Detektor einen zusätzlichen Trennfaktor von etwa 100 durch Ausnutzung unterschiedlicher Energieverlustprofile von $^{44}Ti^{3+}$ und $^{44}Ca^{3+}$. Die kombinierte Unterdrückungsfähigkeit übersteigt potenziell 10^8 und könnte mit Installation des OPO-Lasers 10^{13} erreichen.

Selbst hergestellte ^{44}Ti-Standards zeigten nach Normierung eine Übereinstimmung innerhalb von 40% mit ihren nominellen Werten. Das etablierte Detektionslimit von $1{,}2 \cdot 10^{-13}$ (^{44}Ti/^{48}Ti) liegt etwa einen Faktor 12 über den besten Literaturwerten von $\approx 10^{-14}$, die an größeren 14 MV Anlagen erreicht wurden.

Dies demonstriert die VERA-ILIAMS-Fähigkeit zur Messung von ^{44}Ti-Proben im Bereich von 10^{-13} (^{44}Ti/^{48}Ti), wie beispielsweise existierende Proben aus kernphysikalischen Experimenten am Helmholtz-Zentrum Dresden-Rossendorf (HZDR). Weitere methodische Verbesserungen sind jedoch erforderlich, um die bestmögliche Empfindlichkeit bei VERA zu erreichen. Diese Arbeit legt den Grundstein für zukünftige Untersuchungen der ^{40}Ca(α,γ)^{44}Ti-Reaktion und validiert VERA-ILIAMS als einzigartige Anlage zur Untersuchung stellarer Nukleosynthese durch Präzisionsmessungen seltener Isotope, die zuvor nur an den größten AMS-Anlagen zugänglich waren.

Contents

1. Introduction

The radioisotope ^{44}Ti has garnered significant interest in recent years, primarily due to its surprising discovery in two young supernovae (SNe) remnants, namely SN1987 and Cassiopeia A (Cas A) [1, 2]. With its short half-life of 58.9 ± 0.3 years [3] it can only be found for a few hundred years after a supernova took place [4] and thus offers a momentary insight into stellar nucleosynthesis. As a complete physical understanding of SNe has not yet been achieved, ^{44}Ti can offer new possibilities to benchmark SNe simulations and thus could lead to deeper insights into the process. Additionally, due to its short half-life, ^{44}Ti could lead to new knowledge into century scale solar activity via meteorite analysis [5, 6].

Titanium-44 is primarily produced via the nuclear reaction ^{40}Ca$(\alpha,\gamma)^{44}$Ti. Its measured cross section at the relevant energies around 4.5 MeV however disagrees with observation in combination with supernova models of the last few decades [7]. Gamma-ray studies based on the γ-flux and the distance to Cas A yield a comparatively high amount of produced ^{44}Ti of roughly $(160 \pm 60)\mu M_{\odot}$. This number is higher by a factor of two to ten than what is predicted from SNe models based on cross sections obtained by lab experiments on the reaction ^{40}Ca$(\alpha,\gamma)^{44}$Ti [8].

Attempts to measure the production cross section immediately after the discovery mostly focused on conducting gamma-spectrometry to determine the amount of ^{44}Ti in man-made samples, beginning from $1.8 \cdot 10^{12}$ atoms [9] down to $\approx 6.4 \cdot 10^{6}$ atoms corresponding to a ratio of $\approx 2 \cdot 10^{-13}$ relative to stable Ti in samples from irradiated ^{40}Ca [10]. At amounts below that, the decays may not be detected reliably. Another, possibly more sensitive way to measure ^{44}Ti is via AMS (accelerator mass spectrometry) [9], which allows for individual atom counting and bears other systematic uncertainties. The advantage of this approach is that it is possible to measure smaller amounts of ^{44}Ti than before. At large AMS facilities, a ratio sensitivity of 10^{-14} relative to the stable isotopes was accomplished, which corresponds to roughly $3.2 \cdot 10^{5}$ atoms from a sample where 3 mg stable Ti was added.[7].

The aim of the project is to investigate and advance the detection of ^{44}Ti using the VERA (Vienna Environmental Research Accelerator) facility and to develop AMS methods for later measurements of the cross section of the nuclear reaction ^{40}Ca$(\alpha,\gamma)^{44}$Ti.

As every other AMS facility, VERA uses bending magnets and electrostatic analyzers to separate nuclides of a different mass from each other. Molecules with nearly the same mass as the ion of interest are efficiently destroyed in the stripping process in the accelerator. However, utilizing AMS comes with its own challenges. Isotopes from other elements with the same mass number (an isobar), both atomic and molecular, are the biggest problem. In this case, ^{44}Ca may interfere with ^{44}Ti in the detector thus making the measurement of ^{44}Ti effectively impossible, as ^{44}Ca is stable and orders of magnitude more abundant than ^{44}Ti in a given sample, being also present in dust, sweat and everyday objects.

For this reason, AMS measurements of ^{44}Ti so far have been limited to large AMS facilities providing high ion energies produced by up to 14 MV accelerators [9, 7], allowing ^{44}Ti to be

better distinguished from ^{44}Ca in the detector at a higher energy due to their different energy loss behavior. Unfortunately, all but one of these facilities have meanwhile been decommissioned.

The unique isobar suppression technique ILIAMS (Ion-Laser InterAction Mass Spectrometry) however offers exciting new possibilities for combating this issue at VERA at the Isotope Physics Group of the University of Vienna [11]. It may be possible to detach electrons from the isobaric anions in the ion cooler at ILIAMS by more than the ideally unaffected target nuclide, thus limiting or in the best case eliminating the interference of ^{44}Ca. This may allow for a sensitivity possibly as good or perhaps even exceeding the one in typical literature at $\approx 10^{-14}$ despite the smaller accelerator voltage of just 3 MV. The remarkable additional capabilities offered by ILIAMS compared to other facilities allows us to directly suppress the isobar instead of relying on high energies to separate ^{44}Ca and ^{44}Ti in the detector.

At the beginning of this thesis, the physical and technical basics will be covered that are necessary to understand all further parts such as methods and results, see chapters 2 and 3. Afterwards, all topics that have been investigated in this work will be laid out one by one, including all technical necessities, results and a short discussion for each subject. First, the already existing results from experiments prior to the thesis will be covered in chapter 4.1. From them, it is continued with the general development of measurement methods toward the eventual detection of ^{44}Ti in the remainder of chapter 4. This includes experiments on yield, isobar suppression, ideal sample material and estimations of the separation in the detector. Then, the focus will shift to preparations and tests in the order of their necessity for the final measurement of ^{44}Ti, beginning with chemistry and sample preparation in chapter 5. Lastly, chapter 6 explains blank measurements followed by the measurements of in house produced ^{44}Ti samples from material sent by the PSI in chapter 7. At the end, a brief conclusion and outlook are offered in chapter 8.

2. AMS Techniques

2.1. Accelerator mass spectrometry

Accelerator Mass Spectrometry in most basic terms is the counting of atoms using two mass spectrometers with an accelerator in between [12]. The samples described in later chapters have all been analyzed using this technique. AMS aims to detect the lowest amounts of a given radioisotope within a larger sample, relative to stable isotopes, utilizing the mass of the atom in question and the molecules it can form with e.g. oxides or fluorides. Through energy and momentum 'filters' it is possible to achieve this task.

Typically, as an ion leaves the source, its energy lies between 30 to 70 keV. The accelerator attracts the incoming ions with it's high potential, strips electrons from them and breaks up molecules, only letting atomic ions go past it, thus effectively splitting the whole setup in two, see Figure 2.2. After it, the ions are again accelerated to 3 MeV as they now have positive charge. The side before the accelerator is referred to as the 'low energy' side, and subsequently after the accelerator is called the 'high energy' side. By only allowing ions to pass with a specific mass over charge ratio before and doing the same after the accelerator, influences by other ions, molecular or atomic, of a similar mass over charge are kept to an absolute minimum. In the case of e.g. $^{48}Ti^{3+}$, $^{16}O^{+}$ has a very similar mass over charge ratio and could thus potentially cause problems.

Measuring the absolute amount of any given isotope is virtually impossible. All characteristics about the facility would have to be known in great detail for a specific isotope to measured in absolute terms. The transmission through every part of the facility, the exact yield out of the cathode, chemical purity of the material as well as an exact assessment of any handling and the introduced contamination would need to be carried out.

In order to avoid such efforts for any given measurement, the ratio of the radioisotope to the stable isotope(s) are measured relatively. The current of the stable constituents are easily measurable in an FC and adding stable carrier to an existing pure sample requires only little effort in comparison. The stable part in case of VERA is measured after the accelerator in FCs downstream of the first HE bending magnet. Both stable and radio nuclides are measured at a various times after one another to compensate for source fluctuations. Since the transmission for them will not be the same between different nuclides, a standard is needed to correct the measured counts of the radionuclides.

Sputter source

Both sources at VERA are cesium sputter sources, more specifically MC-SNICS(Multi Cathode Source for Negative Ions by Cesium Sputtering).

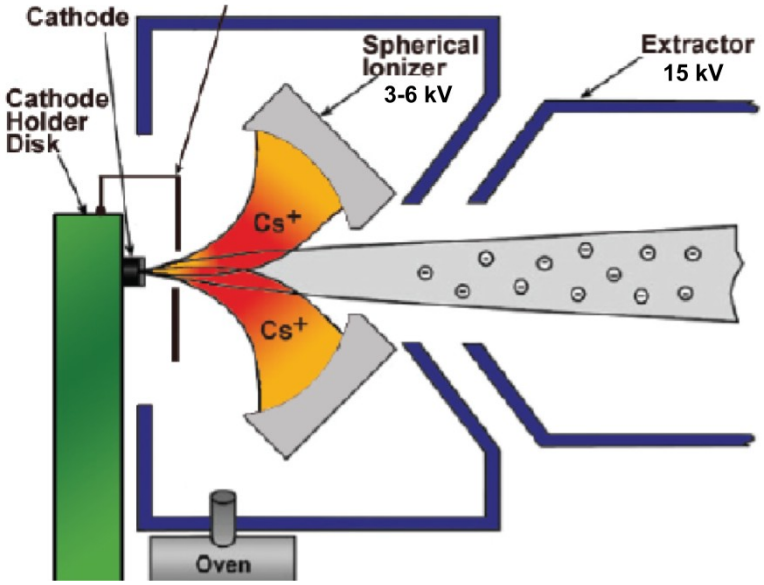

Figure 2.1.: A scheme of the MC-SNICS ion source at VERA, taken from the manufacturer [13].

Figure 2.1 shows a scheme of the MC-SNICS source installed at VERA (for details on the SNICS source see e.g. [14]). Cesium vapor is released from an oven into a sealed chamber between a cooled cathode and a heated, spherical ionizer. The high temperature of the ionizer's surface causes cesium atoms to become thermally ionized. Simultaneously, some neutral cesium vapor condenses onto the face of the cathode. The newly created positive cesium ions are accelerated toward the negatively charged cathode. Their impact sputters particles from the cathode material through the thin layer of condensed cesium. This sputtering process generates mostly neutrals, but importantly some negative ions, which are then accelerated away from the cathode and back toward the positive ionizer. Due to the applied ionizer potential of around 3-6 kV at the source, ions of the sample leave the cathode. This technique allows for a mostly constant current of ions (around 700 nA in the case of TiO^-) out of the source with relatively few fluctuations as the sources are able to regulate some of their parameters, trying to keep the current reasonably constant.

To avoid charges on the sample itself getting too large and unstable for measurements, a metallic binder is added to insulating sample materials, in the case of TiO_2 samples it is silver powder. The optimal ratio of sample to binder material is tested later.

Electrostatic analyzer (ESA)

The ESA is one of the 'filters' mentioned earlier. It filters for the energy over charge (E/q) ratio of the atom in question. Energy filters are necessary to have after the ion source and in the high energy beamline to later eliminate ions of other masses that may have gotten the right momentum by chance. This is achieved by having two charged surfaces at different potentials at a constant radius in a bend. For a charged particle under the influence of an electric field, the deflection

calculates as follows:

$$r = \frac{2Ed}{qU} \Rightarrow rU = \frac{2Ed}{q} \tag{2.1}$$

where in equation 2.1, r is the deflection radius, E is the kinetic energy of the incoming particle, d is the distance between the two electrodes of the ESA. q is the charge of the particle and U is the potential difference of the charged electrodes. Given a constant values of r and d, which are given by the construction, the ESA will filter particles in accordance with their E/q ratio at a given voltage.

Bending magnet (BM)

The magnetic field of the BM is perpendicular to the plane on which the particles move in the facility. It serves a similar purpose as the ESA, just with the momentum over charge (p/q) ratio. A BM at VERA really is a dipole electromagnet, using copper coils and an iron core to create an adjustable, strong, and homogeneous magnetic field. In between two of these yokes lies the beamline in a rectangular chamber to assure ideal geometry with respect to the magnetic field. For this case, the formula for the deflection in a magnetic field can be expressed as:

$$r = \frac{\sqrt{2mE}}{qB} \Rightarrow rB = \frac{\sqrt{2mE}}{q} \tag{2.2}$$

Note that in equation 2.2, $\sqrt{2mE}$ is equivalent to mv, or the momentum p of the particle, where m is the mass of the ion. In other words, the BM filters the particles due to their p/q ratio at a fixed r and magnetic field B.

Taking into account the ESA and the BM after another and introducing that the velocity $v = \sqrt{\frac{2qV}{m}}$, where V is the voltage of the pre-accelerator and keeping in mind that $E = qV$, it can be seen that

$$\frac{mv}{qB} = \frac{2Ed}{qU} \Rightarrow \sqrt{\frac{m}{q}} = \frac{Bd\sqrt{2V}}{U} \tag{2.3}$$

As is evident from eq. 2.3, ESA and BM in total sort the $\frac{m}{q}$ ratio of ions, enabling mass spectrometry.

Faraday cup (FC)

Faraday cup is an insulated metal cup that allows to measure all the current of the ion beam if put in the beamline. The cups serve two purposes, first to stop the current from going any further into the facility, e.g. for protecting sensitive detectors and secondly to measure the current at a given point making them very valuable during tuning.

With this said, the FCs are limited in sensitivity as the lowest detectable current is generally around the pA range. A pA of $^{44}Ti^{3+}$ are around $2.1 \cdot 10^6$ ions per second, which are already more ions than the detector can count in a second.

Tandem accelerator

VERA utilizes a 3 MV pelletron with two chains delivering a terminal voltage. As the incoming negative ions are attracted to the positive potential they collide with the so called stripper gas (typically helium or argon) that is located in the center of the tandem accelerator, which breaks up the molecules into its constituent atoms, leaving them with positive charges since some electrons are stripped off. These atomic ions are now repulsed by the positive charge of the central terminal and accelerate away back to ground, further down the beamline.

The energy after the accelerator is dependent on the charge of the ion after the stripping process as well as the injection energy, the ratio of mass after to before the stripper and the terminal voltage of the tandem accelerator. As a formula, this can be expressed as:

$$E_H = (E_i + q_L \cdot U_{\text{terminal}}) \cdot \frac{m_H}{m_L} + q_H \cdot U_{\text{terminal}} \tag{2.4}$$

In equation 2.4, the index $_L$ is used for the low energy side before the accelerator and the index $_H$ is used for the high energy side after the accelerator. E_i is the initial energy of the incoming particle at the tandem accelerator, q_L is its charge and U_{termnial} is the terminal voltage of the accelerator. m_H and m_L denote the masses of the particle, as it breaks up in the stripper.

Gas ionization detector

In order to detect the now positively charged atomic ions on the high energy side after the accelerator and more kinematic filters, the energy loss inside the gas of the ionization chamber in the detector is used. When ions enter the detector through a thin silicon nitride window, they travel through a pressurized isobutane gas where they gradually lose energy via ionization interactions with the gas. The detector's volume spans about 6 cm in length and features a split anode design with two consecutive regions of equal length, allowing simultaneous measurement of energy loss in different sections, usually expressed as δE_1 and δE_2 or δE and δE_{res}. A Frisch grid made of tungsten wires ensures uniform electric field conditions, while voltages of 200 V between anode and cathode cause the separation of the charges after ionization. The key to the detector's effectiveness lies in particle identification through differential energy loss patterns. Different isotopes, even those with the same mass number, exhibit slightly different stopping powers in the gas due to their distinct nuclear and electronic properties. By measuring both the energy loss in the first region and the residual energy in the second region, the system creates characteristic signatures for each particle type. The charge-sensitive pre-amplifiers, mounted directly inside the detector volume to minimize electronic noise, convert the ionization signals into measurable voltage pulses that are then processed by spectroscopic amplifiers and digitized for analysis. This approach enables the suppression of unwanted isobaric interferences that plague accelerator mass spectrometry measurements. For example, the detector achieved suppression factors of $3 \cdot 10^4$ for ^{36}S interference in ^{36}Cl measurements and even more for others [15].

Separation in the detector

To distinguish between two atomic ions in the detector, they need to behave differently in terms of δE_1 and δE_2. This can be achieved at larger accelerator facilities with terminal voltages up

to 14 MV by scaling the small differences in energy between isotope of interest and isobar. The difference in stopping power of the two atoms is different enough to distinguish them [7, 16]. At VERA, 3 MV terminal voltage may not be enough to fully accomplish this goal, possibly only partially separating the two regions of interest in the detector.

2.1.1. Implementation at VERA

As apparent from figure 2.2, the components mentioned before are not exhaustive by any means. In principle, VERA consists of one mass spectrometer before and one after the accelerator itself. Starting from source 2, negative ions are produced by the SNICS source, sputtering material from the sample. The ion beam then passes through a series of BMs, that selects for a specific mass to charge ratio, and ESAs, which filters ions by their energy to charge ratio, followed by a double-focusing injection magnet. The filtered beam enters a 3 MV Tandem Pelletron accelerator, where negative ions are first accelerated toward a central stripper gas region. There, molecular ions are broken up and electrons are stripped, converting the ions to positive charge states. The now positive ions are accelerated again through the second half of the accelerator. On the high energy side, a second magnet and ESA again filter by mass to charge ratio. Due to the ambiguity of this selection, mass over charge interferences, e.g. by stable isobars, inevitably remain in the beam alongside the radionuclide of interest. To address isobar suppression at lower ion energies, where detector based separation becomes insufficient, VERA introduced the ILIAMS setup in 2016.

ILIAMS

ILIAMS (Ion-Laser InterAction Mass Spectrometry) is a technique developed at the VERA facility to suppress isobaric interferences. Installed in 2016, it functions as an additional selective element placed after ion source 2 (see Fig. 2.2). Its core function is to remove unwanted ions (isobars) through the process of laser photodetachment and collisional interactions with the gas, allowing the desired ions to pass through (mostly) unaffected for subsequent AMS analysis.

Figure 2.3 shows the second ion source at VERA with the subsequent ion cooler and the laser setup, which in total is referred to as ILIAMS. As a unique facility, it presents the main suppression venue that is going to be used in the course of this work. The key component is an ion cooler, which is a linear radiofrequency (RF) quadropole ion guide. Negative ions are extracted from the source, separated by momentum/charge in a magnet, and then injected into this cooler. To enter the cooler, the ions are first electrostatically decelerated to energies of around 45 eV. The ion guide itself is filled with a buffer gas, typically helium at a low pressure of around 4 Pa. The RF field creates a potential that confines the ions along the axis, while collisions with the light gas atoms efficiently cool and thermalize the ion beam, reducing their kinetic energy to less than 1 eV while also focusing them. This cooling is crucial as it dampens the ions' motion and increases their interaction time with a collinear laser. The guide also acts as a weak mass filter; for a given RF setting, it only transmits ions within a specific mass range, filtering out others [18].

The fundamental process used for separation is photodetachment, described by the equation $A^- + \gamma \rightarrow A + e^-$, where a photon ($\gamma$) knocks an electron off a negative ion. This is a threshold

process, meaning it only occurs if the photon energy (E_γ) exceeds the electron affinity (EA) of the ion. Inside the gas-filled ion cooler, the cooled ion beam is overlapped collinearly with a continuous laser beam. The laser's photon energy is carefully chosen to be higher than the EA of the unwanted isobar but lower than the EA of the isotope of interest. Consequently, the unwanted ions absorb the photons and are neutralized via photodetachment, while the desired ions remain unaffected. The efficiency of this depletion depends on the photodetachment cross-section (σ), the laser photon flux (Φ), and the interaction time (t) inside the cooler, following the relationship

$$N_{depleted} = N_0(1 - e^{-\sigma\Phi})$$

The long, ms-scale interaction time achieved in the cooled, guided beam enables a suppression efficiency of >99.99% for the unwanted isobars.

Usually, a range of lasers are the main suppression tools at ILIAMS. Those lasers range from the infrared to UV. The UV laser sits at 355 nm (3.5 eV), a green laser also available at 532 nm (2.3 eV), a red laser at 637 nm (1.9 eV) as well as a tunable titanium-sapphire (TiSa) laser between 675 nm (1.8 eV) and 1100 nm (1.1 eV) that was not available yet at the majority of the time during this work. There is also an infrared laser with a longer wavelength that was not tested.

Furthermore, the buffer gas in some cases itself aids in suppression through collisional detachment and chemical reactions. This effect can be enhanced by mixing gases like O_2 into the helium [18]. A critical requirement is that the ion's energy upon entering the cooler must be managed carefully. The maximum allowed energy is determined by the need to prevent collisional detachment of the desired ion; the center-of-mass energy of an ion-gas collision must be lower than the electron affinity of the ion of interest to ensure its survival. Additionally, a critical requirement is that the ion's phase space upon entering the cooler must be managed carefully. This includes not only the beam energy but also the energy spread and angular divergence.

2.2. Samples and measurement procedures

Blanks

When investigating the measurement of a radionuclide at AMS facilities, the biggest obstacle is usually the isobar and contamination with it from handling and/or the environment. To test how much isobaric contamination there is without the actual radionuclide present, blanks are put to use. Blanks are sometimes divided into machine blank and processing blank where a machine blank is the best attempt of introducing no isobar at all, while the processing blank runs through the same steps as other samples to gauge the amount of contamination introduced through handling. No machine blanks are used in this thesis, and the term blank refers to processing blanks from here on.

Blanks are used in this thesis to establish the background of ^{44}Ca and ^{44}Ti that is introduced during sample preparation, specifically the chemical preparation described later in section 5.2. Ideally, the ratio of $^{44}X/^{48}$Ti induced by ^{44}Ca will be as low as possible, with literature currently residing at $\approx 10^{-14}$ in terms of blank levels [7, 19].

In order to get the isotope ratio, the counts in the detector are compared to the calculated counts of $^{48}Ti^{3+}$ on the HE side in cup MFC 04 from the respective current.

$$\frac{^{44}X^{3+}}{^{48}Ti^{3+}} = \frac{cps \cdot 3e}{I_{HE}} \tag{2.5}$$

In equation 2.5, I_{HE} stands for the HE current, *cps* are the counts per second in the detector and e is the unit charge. Note that the whole HE side is charged 3+. Test of the blanks used in preparation to the measurements of ^{44}Ti can be found in section 6.

Standards

While the blank level is an important quantity to know, samples that contain ^{44}Ti are equally important. Since we cannot carry out an absolute measurement, it is paramount to have some sort of correction mechanism.

A standard has a known ratio between the radionuclides and its stable counterparts. If this standard has been measured in other facilities previously or is some sort of established industry standard, it is sometimes referred to as a "primary standard". It must be noted here that there is no widely used or accepted primary standard available for ^{44}Ti as there has been no AMS measurements of it in many years and the amount of existing ^{44}Ti at the HZDR for example is somewhat under contention [20].

All standards mention hereafter are not to be seen as primary standards, but in-house standards with known compositions whose ratio have been calculated. The in-house standards are prepared by a dilution series, which are consecutive dilution steps from one base solution to minimize handling and to have one initial base solution to possibly repeat measurements. In total, four dilution steps have been carried out, their ratios of ^{44}Ti/^{48}Ti ranging from $5{\cdot}10^{-9}$ to $5{\cdot}10^{-12}$.

In practice, multiple cathodes per standard are prepared. For the sake of this example, only three cathodes of a single standard are being discussed. This standard has an isotopic ratio of X, and its measured ratio after sputtering is Y. In order to correct e.g. the blank or eventually samples from meteorites, a correction factor of Y/X is applied to all cathodes.

In reality of course, multiple standards are measured. Usually the normalization is carried out against the highest standard, as it is typically the one that was handled the least and for which the counting statistics are best. The hope after measurements is that all cathodes of one standard are close together and that the standards after normalization are reasonably close to their nominal ratios.

As ^{44}Ti is not abundant in nature due to its short half life and its seemingly rare production in SNe, getting actual ^{44}Ti for investigation was only possible by artificially producing ^{44}Ti. The Paul Scherrer Institute (PSI) offered 2.5 kBq ^{44}Ti to be sent to us as a contribution to scientific progress on that matter. Even more fortunate, the actual activity produced was closer to 12 kBq, specifically (12.05±0.25) kBq, allowing the conduct of more extensive tests than initially thought. Please note here that the uncertainty given here is only that of the counting statistics. No error budget of sample handling or chemistry was provided. The chemistry and handling of the standard material can be found in section 5.

The reaction with which ^{44}Ti was produced at the PSI was not however done via ^{40}Ca(α,γ)^{44}Ti as is typically the case. To avoid excess amounts of Ca that would possibly obstruct solid results from additional counts from ^{44}Ca, the reaction ^{nat}V(p, X)^{44}Ti was utilized instead. This reaction takes place at around 147 MeV and has a cross section close to 804 μb [21].

It is important to underline here that the goal of this thesis is not the measurement of irradiated targets via $^{40}Ca(\alpha,\gamma)^{44}Ti$ but the feasibility and development of measuring ^{44}Ti by with VERA and ILIAMS.

Note that the names of all the standards, SMV-Ti-XX is composed of the responsible chemist, Silke Merchel and was prepared in Vienna. Ti of course stands for titanium and the two numbers indicate the order of magnitude of ^{44}Ti/stable Ti.

Spikes

Some isotopes require an isobar spike to measure. A spike is a deliberate addition of either a specific isotope or element far above their abundance in samples or what is introduced during handling. No such spikes are strictly necessary for the steps to measure ^{44}Ti explained here, but valuable lessons may be learned from an isobar spike with small (0.1% to 0.005%) amounts of CaO and are thus used in this work. Large amounts of CaO cannot be introduced, as previous tests have shown it to poison the ionizer, i.e. reduce the ionization capability for Cs on the hot surface.

A correction is carried out with the Ca-spikes. Counts in the region of interest of $^{44}Ti^{3+}$ are put in relation to the total number of Ca counts, such that an estimate is gained about how many atoms out of a given amount of Ca will make it into the Ti region of interest. With this known quantity, all samples can be corrected, but most importantly, the blanks are corrected with this method.

HZDR ^{44}Ti samples

The Helmholtz Zentrum in Dresden Rossendorf (HZDR) has prepared irradiated ^{40}Ca samples in 2012. If 1 mg of ^{48}Ti was added to the existing samples, the ratios would lie between $\approx 3 \cdot 10^{-12}$ and $\approx 4 \cdot 10^{-14}$ [20].

As these targets are readily available at the HZDR and are well documented, a AMS measurement could complement the partially disagreeing γ measurements carried out at the PSI, the Felsenkeller lab and the HZDR. If those targets could be measured at VERA, a cross section for astrophysically relevant energies could be established and compared with the existing one of roughly 8 μb over the relevant energy ranges [7]. It should be noted that these samples have not been measured during the course of this work.

Typical procedure

Typically, a blank, multiple standards and possibly a few spikes are measured in one beam time, along with cathodes for tuning and old C targets[1] for regenerating the ion source and diagnosis should any problems arise.

During the course of a measurement, the facility alternates between measuring stable currents and counts in the detector on its own. Usually, the current is measured in a FC for five seconds, after which the counts are recorded in the detector for 100-200 s. In total, four current and three count measurements in between the current measurements comprise one so called “run”.

[1] Cathodes that have been used to measure ^{14}C for commercial use that are still relatively full

The current of the stable isotope is measured before and after each measurement period of the radionuclide counts in the detector. In practice, the average of the current is typically assumed and results are calculated with it as the difference in current between two measurements withing the same run usually does not exceed a few percent. A more detailed description and list of available lasers at VERA can be found at 2.1.1.

In a typical beam time, starting currents in FCI 1-1 (before the cooler) usually lay around 150 nA to 200 nA, which start decreasing after about 40 minutes and continue to do so until the cathode is empty around 5-6 hours later for 3 mg material. After the cooler in MFC 2-2, currents typically average around 50 nA with He in the ion cooler at 5 Pa. A detailed trend of the current for a typical beam time can be seen in 4.6. These typical currents are obtained with source parameters similar or equal to the ones found in table 4.1.

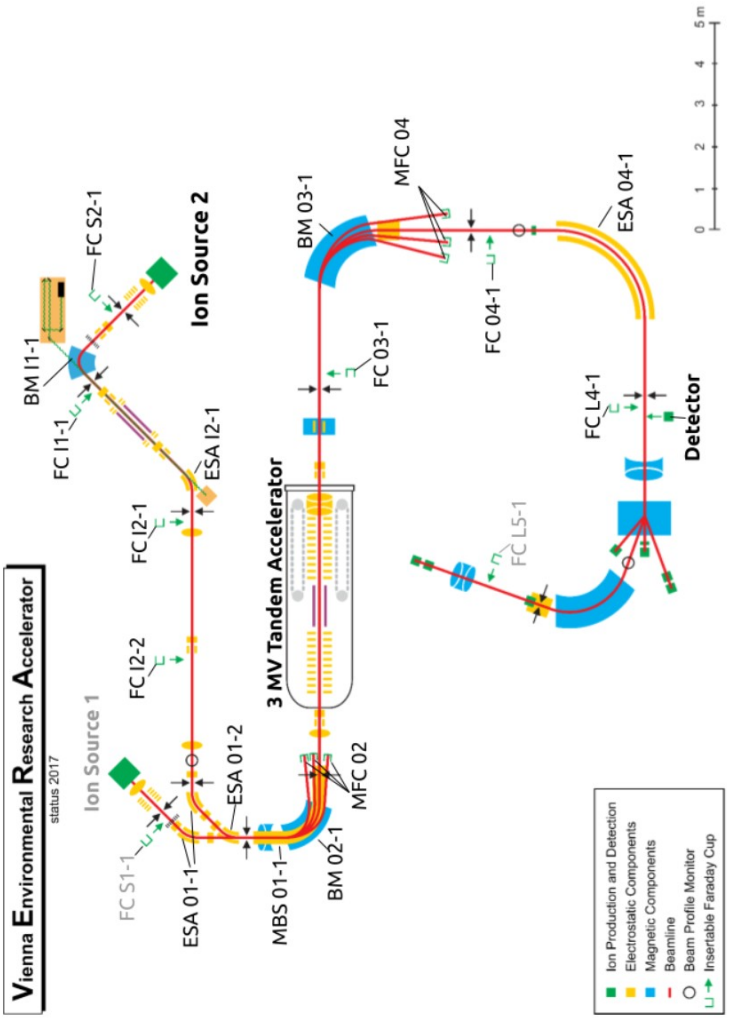

Figure 2.2.: The setup at VERA as of 2021, taken from [17]. Note that since this scheme, small changes have been made that do not change the overall mechanism or procedure of this work. The mass spectrometer in front of the accelerator sorts the molecular/atomic ions on the low energy side and the one on the high energy side is sorting the atomic ions of the remaining. The blue elements in figure 2.2 are magnetic elements, where the orange one are electrostatic. The beam line is red and green is reserved for the origin (ion source) and destinations (FCs and detector) of the beam. This image acts as a reference for later descriptions. Irrelevant parts for the experiments described herein are labeled in gray.

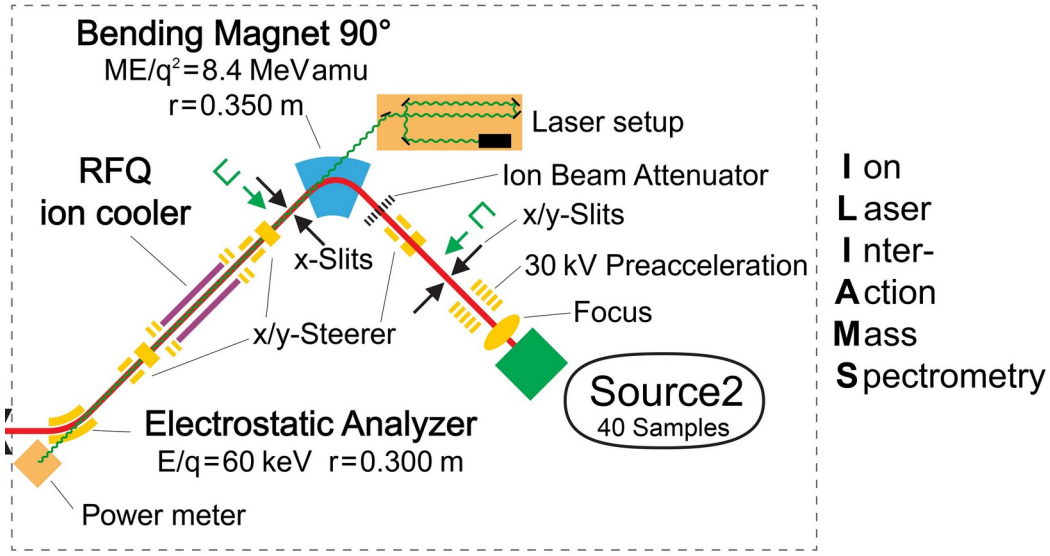

Figure 2.3.: A more detailed description of ILIAMS, where the main suppression takes place with the laser and the ion-gas interactions in the RFQ ion cooler.

3. ^{44}Ti in the Universe

Since titanium is a relatively light element, with an elemental mass of 47.87 g /mol, its primary production process is the capture of alpha particles by calcium nuclei during supernovae. The rare isotope ^{44}Ti is significantly produced there as well, particularly during the freeze out stages of a specific type of supernova, as laid out in more detail in 3.1.

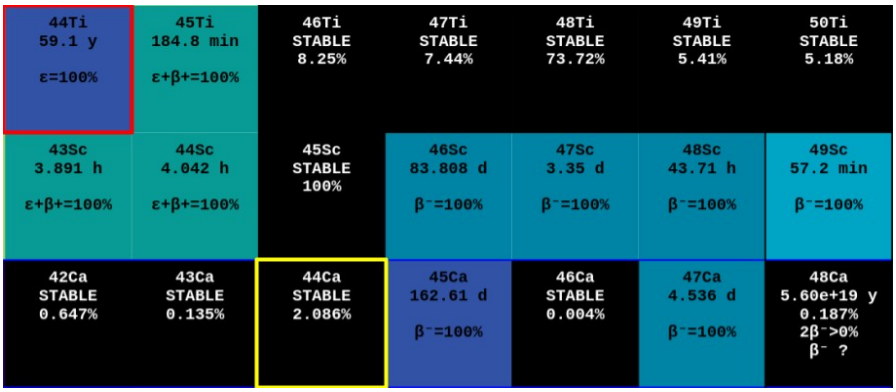

Figure 3.1.: A section of an isotope chart showing ^{44}Ti enclosed in a red box and ^{44}Ca enclosed in a yellow box and the five stable isotopes of titanium, ^{46}Ti to ^{50}Ti. This image was taken from https://www.nndc.bnl.gov/nudat3/ and was retrieved on the 18th of June 2025.

^{44}Ti is not abundant on Earth due to its short half life. Any amount that may have been here from some supernova remnant has long decayed and can no longer be found. The only exception to this are the few artificial samples created for specific measurements [7, 20].

3.1. Core collapse supernovae and ^{44}Ti production

During the life of a star, heavier elements are produced via nuclear fusion from hydrogen. Helium is the first to form after fusion starts, and as the star ages, various elements form in shells around the core of the star. More massive elements form further inwards, such that the final star at the time of its supernova[1] has the following shells from the core outwards: Fe/Ni, Si, O, Ne, C, He, H[2].

[1] Or at least for this specific kind of supernova

[2] Only listing the primary element of the shell without any fractions of co-products.

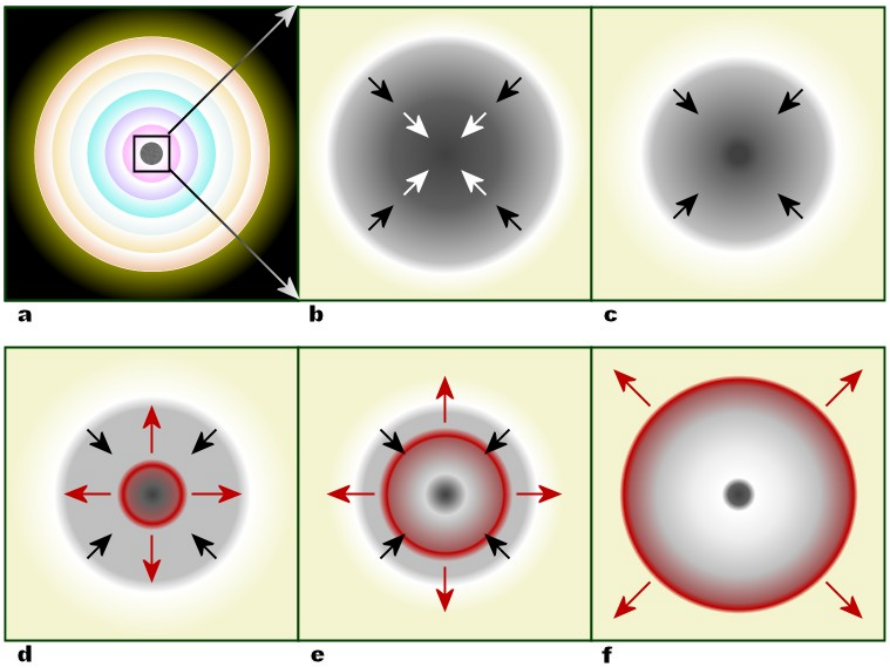

Figure 3.2.: A schematic overview of the stages of core collapse supernovae. (a) shows the star in its latest stage of life, (b) depicts the iron core, (c) shows that part of the core being compressed to neutrons and causing the first expansion (d). (e) shows the outward moving shock front in red and the rest of the infalling material that is finally picked up and also expelled (f). This image was taken from [22].

At the end of it's life, depending on it's exact mass, a main sequence star experiences one of multiple types of supernova. Core collapse supernovae, also known as supernova Type II, are towards the higher mass end of typical main sequence stars, $>8M_\odot$ and $\lessapprox 25M_\odot$ [4].

During the Type II SN, after the mass of the core has exceeded its ability to exert force on upper layers via fusion, gravity forces material inwards until it cannot be further compressed. This compression forces the inner material to turn into neutrons. This core collapse happens incredibly rapidly, taking only milliseconds as the iron core reaches the Chandrasekhar limit and can no longer support itself against gravitational forces. The resulting neutron core becomes extremely dense, about 10^{15} grams per cubic centimeter, creating a rigid surface that causes the infalling material to bounce back and generate the explosive shockwave. The outside part of the core and a large part of the shell get propelled outwards from the shockwave of infalling material. It is during that phase that a vast particle flux forms many new elements via capture by shell material from the former star. This process is depicted in figure 3.2.

As the shockwave travels through the Si rich layer of the star, nuclei are exposed to high temperatures and can start to break, emitting α particles [23]. In the case of ^{40}Ca(α,γ)^{44}Ti, α particles hit expelled Ca, likely around the resonance of $\approx$4.5 MeV. The exact conditions in which this occurs are not well known and are the topic of current improvements to SN modeling [19, 4, 8].

Some of these processes, particularly at E_α<3 MeV, are poorly studied with only upper limits for resonance strengths [7, 24]. in laboratories and may show resonances at specific energies, further complicating any estimations of these reactions.

If the product of such reactions could be reliably measured, actual cross sections could be evaluated in laboratories like VERA after irradiation in other facilities. Through this, insight could be gained into some of the more illusive processes of nucleosynthesis and corrections may be applied to current models, adding to our understanding of the topic.

Furthermore, if Ti lines are only found in some specific SNe and the conditions of those SNe are established better, they may be used as some sort of 'standard environment' for other reactions as well. For ^{44}Ti specifically, it's scarcity in SNR hints at some apparently rare conditions at which the reaction happens most efficiently. Schmidt et al.[19] speculate that the necessary energy for the observed lines of SN1987 and Cas A would necessitate a temperature of > 3.5 GK. A small amount of ^{44}Ti is also be produced during O-shell and Si-shell burning [25]. The cross section of the main production avenue ^{40}Ca(α,γ)^{44}Ti is the subject of ongoing debates [9, 16], with the typical value at $\approx$8 μb for the relevant energy range between 0.58-1.16 MeV/u [16].

The tell-tale signs of the presence of ^{44}Ti, namely the γ-lines characteristic of its decay, have been detected first with COMPTEL [2], but later also with other instruments and also lines from decay products of ^{44}Ti [26, 27, 4]. From the amounts of ^{44}Ti it is possible to refine supernova models that in turn may yield more exact predictions and insight into current questions of nuclear physics.

It should be noted here that ^{44}Ti can not be found in most supernovae, as mentioned by [28] or [16]. The two more prominent occurrences of ^{44}Ti in literature are Cas A and SN 1987 [2, 29, 4], although the X-ray detections in the later is still somewhat a topic of discussion. [4].

Studies based on γ-fluxes and the distance to Cas A result in a higher amount of ^{44}Ti (roughly $(160\pm60)\mu M_\odot$), exceeding the expected amount from SNe simulations by a factor of two to ten. γ-ray and AMS measurements of the reaction ^{40}Ca(α,γ)^{44}Ti also disagree with SNe simulations, but line up well with the highest yield range of new SN simulations [7, 16, 8].

^{44}Ti in meteorites

Galactic cosmic rays (GCRs) cause the production of some radionuclides outside of their typical production mechanisms in SNe. These radionuclides can also form on the surface of meteorites and in dust grains. Thus, such deposits can be used to track GCR activity and influencing effects such as sun spots, as the sun acts as a shield for galactic cosmic rays [5].

Due to its short half life ^{44}Ti could be used as a tracer for century-scale GCR activity, as it is likely created in iron and nickel from high energy (>70 MeV) rays [6]. An anticorrelation between sunspot number (and thus solar activity) and ^{44}Ti activity has been measured. Note that the concentration of ^{44}Ti in meteorites is very low, at best measuring 0.1 Bq/kg [6].

3.2. A brief overview of ^{44}Ti in astrophysics

The initial discovery of ^{44}Ti using COMPTEL aboard the Compton Gamma Ray Observatory (CGRO) carried out by Iyudin et al. [2] showed evidence of an emission line at 1.157 MeV of

the decay chain ^{44}Ti → ^{44}Sc → ^{44}Ca with about 4σ confidence [2]. The amount of ^{44}Ti in the SNR is estimated to be in the order of $2.3 \cdot 10^{-4}\ M_{\odot}$, an approximate value for ^{44}Ti that has not changed much with consequent observations that center around $1.4 \cdot 10^{-4}\ M_{\odot}$ [2, 4]. While the observations at the time fit into nucleosynthesis models, corrections of some of the nuclear and astronomical assumptions since then have led to a lack of ^{44}Ti from SN simulations.

The et al. followed with Cas A observations using the Oriented Scintillation Spectrometer Experiment (OSSE on CGRO), the detection of ^{44}Ti could be reproduced within reasonable deviation [1]. It is also noted that the measured amounts of ^{44}Ti fit reasonably well with current SN models of the time. This changed with advances in SN modeling, leading to the so called "missing ^{44}Ti problem". Following the initial discovery of ^{44}Ti in SNR, the question of potentially measuring samples was raised quickly. Hui et al. [9] used AMS for the first time to measure ^{44}Ti directly. An experiment was conducted at the Koffler 14UD Pelletron, managing to demonstrate a sensitivity of $\approx 10^{-14}$ for ^{44}Ti/^{stable}Ti. Titanium-44 was produced by ^{12}C(^{34}S,2n)^{44}Ti for its ease of production compared to ^{40}Ca(α,γ)^{44}Ti or similar reactions. The reaction was realized by a 121 MeV beam of $^{34}S^{10+}$ irradiating a chamber filled with C_4H_{10}. For measurements, a ^{44}Ti source with around 430 Bq activity was used which was chemically prepared in the form of TiO_2. The primary isobar ^{44}Ca was, due to the high acceleration voltage of 12.1 MV, not a problem, as it was well separated in the a gas filled magnet detector.

Paul et al. [10] carried out the first investigation of the reaction ^{40}Ca(α,γ)^{44}Ti by counting ^{44}Ti instead of decay measurements at the Koffler Tandem Accelerator. The target was prepared at the Argonne National Laboratory with their 14 MV accelerator via ^{40}Ca(α,γ)^{44}Ti from a ^{40}Ca beam [10]. A He-target was irradiated with a ^{40}Ca beam, yielding ^{44}Ti in small amounts, about $\approx 6.5 \cdot 10^{6}$ atoms.The corresponding concentration in the target amounted to roughly $1.7 \cdot 10^{-13}$ compared to stable Ti in the final sample.

Nassar et al. [7] studied the average cross section of the reaction ^{40}Ca(α,γ)^{44}Ti for the astrophysically relevant energies from 2.1 MeV to 4.2 MeV and found it to be roughly 8 μb with AMS measurements. They also noted that with this number, the observed amounts of ^{44}Ti in CAS A may make more sense with established SN models than estimations before.

In comparison to estimations using supernova models at that time, the measured cross section is higher by a factor of roughly 5-10 [7, 16] and was thus responsible for a readjustment of said models. The measurements themselves have been carried out using two different 14 MV accelerators. First was the ATLAS linac at the Argonne National Laboratory with the electron-cyclotron ion source to measure specific resonances. Secondly, the Koffler Tandem accelerator was utilized for some samples on a broader energy range to get the integrated cross section. In order to improve the accuracy of previous measurements Vockenhuber et al. [28] used the recoil mass spectrometer DRAGON at TRIUMF-ISAC in Vancouver, Canada to measure ^{40}Ca(α,γ)^{44}Ti, coming out with a result in disagreement with that of Nassar et al. [7], but with less uncertainty [28]. The significantly higher yield stands in contrast to prompt gamma-ray studies conducted previously, the results of which have been used in SNe models, leading to under-prediction of ^{44}Ti in said models.

From this measurement the cross section of ^{40}Ca(α,γ)^{44}Ti is known so precisely that the somewhat lesser known reactions ^{44}Ti(α, γ)^{48}Cr, ^{44}Ti(α, p)^{47}V and ^{45}V(p, γ)^{46}Cr laid out in [30] contribute the highest uncertainty in models when assessing the amount of ^{44}Ti [28]. Hoffman

et al. [31] focused on the previously poorly known resonance strengths of ^{40}Ca(α,γ)^{44}Ti at 4.13 MeV, 4.54 MeV, and 5.36 MeV with the goal of assessing the stellar reaction rate with this new information [31]. The measurements were carried out by bombarding a solid, thick CaO target at the 10 MeV Lawrence Livermore National Laboratory with α particles and measuring the yield via in-beam γ spectroscopy and offline decay counting after the irradiation, yielding lower amounts of ^{44}Ti than would be predicted from theory [31]. Going into even more detail, the exact resonance strengths of ^{40}Ca(α,γ)^{44}Ti at $E_\alpha \approx 4.5$ MeV have been determined by Schmidt et at. [20, 19]. These 4.5 MeV are actually three resonances at the lab frame energies E_x = 9215 keV, 9227 keV, and 9239 keV, which have a significant influence on the total cross section at typical energies in core collapse SNe. These energies translate directly to very specific temperature ranges around 3.5 GK during the SNe that have been found be on the upper end relevant for the reaction in question.

The resonances agree with previous studies [28, 19], reducing the uncertainty of them by about a factor of two while disagreeing with AMS measurements as well as recoil measurements [7]. It must be noted that the low energy resonances of ^{40}Ca(α,γ)^{44}Ti have not been reassessed, thus a correction to the overall production rate or cross section is not given. Persisting disagreements like the ones described in this section thus far, particularly between AMS and other measurement methods, show the importance of continued research on the topic. More precise and repeatable experiments on topic may contribute to solving the issue while also laying the ground work for potential applications of ^{44}Ti measurements. The targets that have been made specifically for these experiments at the HZDR are still available and range from roughly 35 Bq to 500 Bq, which could be prepared into samples by adding 1 mg of stable Ti, translating to ratios from $3 \cdot 10^{-12}$ to $4 \cdot 10^{-14}$. In the discussion, they will be compared to present detection limits at VERA.

Current research

After the resonance measurements, interest in the topic decreased while recent research focused less on the actual reaction and its cross section but more on the astrophysical modeling in refining SNe models, coming to the conclusion that the ^{44}Ti 'underproduction problem' is not longer a serious issue for core collapse SN simulations [8]. Observations of SNe remnants (SNR) trying to find more ^{44}Ti have also been made without much success, finding no ^{44}Ti above background levels, at best establishing upper limits [4].

Some have speculated on where ^{44}Ti is located in the SN remnant, noting the high amount of dust surrounding Cas A which was the first detection of ^{44}Ti. This dust is believed to be the result of a slow process of mass loss of the dying star, creating an unusually dense environment that could be a requirement for the formation of large amounts of ^{44}Ti. As this is a rare process, it could be a possibly explanation of the scarcity of ^{44}Ti detections. Titanium-44 itself is thought to be in the larger dust grains as opposed to being spread equally [25]. Recent findings from presolar supernova grains in extraterrestrial material have found evidence of ^{44}Ti via ^{44}Ca excess as well as other radionuclides that are associated with SNe like ^{28}Si and ^{26}Al. The reported ratio of ^{44}Ti/^{48}Ti is up to (2.14±0.14) at the time of formation [32, 33].

Recent developments in SN models

Recent studies suggest that ^{40}Ca(α,γ)^{44}Ti may not be the main production venue of ^{44}Ti, but rather the conversion of ^{45}V and ^{46}Cr back into ^{44}Ti from strong proton radiation [8]. With new models and different mechanisms, ratios of ^{44}Ti/^{56}Ni that match observations of SN1987 have been achieved.

Contrary to previous assumptions, the dominant production reaction of ^{44}Ti in new models involves neutrino-driven winds at lower temperatures <1 GK that yield observed amounts of ^{44}Ti.

Furthermore, longer term simulations extending to 20 seconds after the bounce show up to $2{\cdot}10^{-4}M_{\odot}$ for masses in range with the estimated mass of SN1987, declaring the missing ^{44}Ti problem as solved. The production timescale for ^{44}Ti appears to be significantly longer than for ^{56}Ni which has previously not been taken into account in most models [8].

4. Method Development toward ^{44}Ti Detection

4.1. The status of ^{44}Ti at VERA prior to this work

In literature, the most prominent sample material to create Ti^{q+} ions on the high energy side was TiO_2, likely to its good availability and non-toxicity compared to many other chemicals [7]. The first ever beam-time of titanium already used this for convenience, but other sample mixtures are tested later in section 4.2.2.

Cathode material

A single Ti beam-time before the start of this thesis had been carried out. The goal of this first beam time was to conduct rudimentary yield tests and to assess which cathode material, copper or aluminum, produces stronger and more stable currents throughout the measurement. Note that the amount of material in the cathodes for this beam time has not been weighed exactly, so at best an estimate of the yield can be calculated. The sample material consisted of TiO_2 and Ag in a ratio of 1:2, with individual mixtures in the cathodes weighing 4 mg up to 7 mg[1]. As a first test, ion currents were monitored in FCI 1-1 in the injector beamline of ILIAMS.

The results of this measurement are that Cu cathodes provide more current throughout the beam time, as is obvious from Figure 4.1. Looking at cumulative currents, the copper cathode yields roughly 30-50% more at mass 64. Thus, all future mixtures have been pressed into Cu cathodes. All cathodes of this work have been made from Cu, apart from very few control cathodes when investigating Cu-molecules.

It should be noted that due to the influence from copper tails to each side of ^{48}TiO, the current at mass 64 may have some tailing influence from Cu. This will be discussed in more detail in section 4.2.2. In addition, it can be seen quite clearly that the production of higher oxides is far more efficient with Cu cathodes, up to a factor of around 5.

In terms of negative ion yield, TiO^- showed about 0.5% yield, TiO_2^- resulted in 0.2% yield and TiO_3^- yielded 0.02%. While this is in no way as exact as it could have been with weighed cathodes, it can be safely said that TiO^- is the highest yielding oxide molecule at VERA.

Ideal positive charge state

On the LE side, TiO^- is the obvious charge state for oxides, as twice negative ions do not exist. TiO^{3+} was chosen on the HE side, both in the experiment prior to this work and also at the first beam time of this work, as well as due to practical considerations from equal masses. TiO^{3+} was assumed to have the highest flux, baring TiO^{2+} which would likely have more flux at the energies

[1] Note that 7 mg was described as difficult to press into the cathodes and that mixing with the plastic spatula was also difficult due to TiO_2 forming platelets when exposed to humidity.

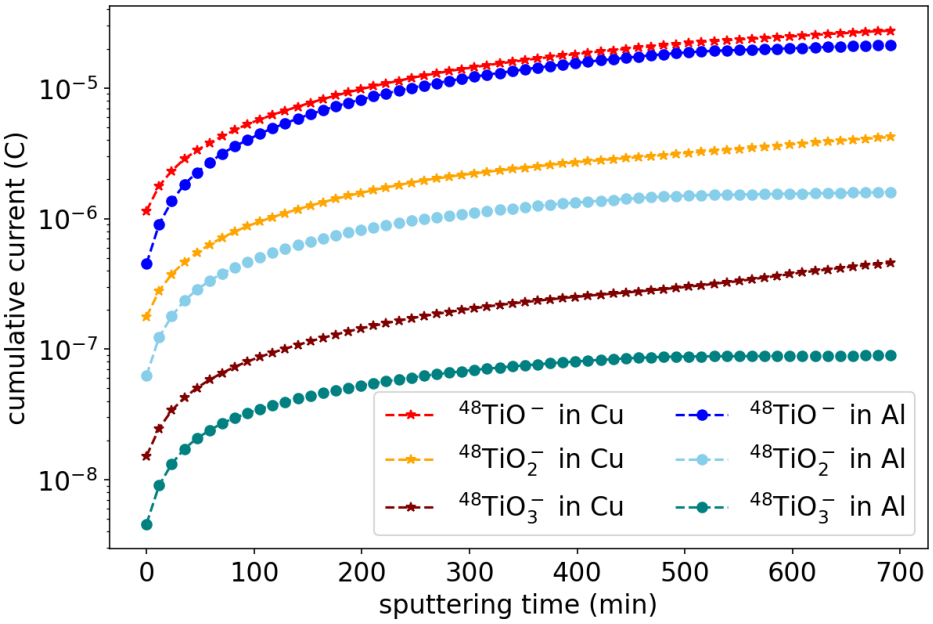

Figure 4.1.: A comparison between two cathodes of tests carried out prior to this thesis. The x-axis shows the sputtering time and the y-axis shows the cumulative current. Note how the copper cathodes consistently produce the higher current throughout all mixtures.

at VERA, but since $^{22}X^+$ would have a very similar m/q ratio than $^{44}Ti^{2+}$, it is dismissed as a possibility.

The stripping gas in the pelletron can also significantly influence currents on the HE side, thus it was also tested what the ideal stripping gas for Ti would be prior to this work. Typically, argon, helium or nitrogen gas are utilized for this purpose. In our case helium was used for most of the tests unless specified otherwise. During tests with argon, the transmission was almost half (10%) of what was achieved with helium at the same time (18%). Due to the poor transmissive performance, Ar was dismissed as a possibility prior to the experiments of this work and was remeasured to be sure yielding similar results. Helium gas with added oxygen in a ratio of 30 /1 yielded a slightly worse transition at about 14-15%, although this was tested in a later experiment.

Summary of the status before this work

In conclusion, before the start of this work, the ideal cathode material, Cu, was determined; the so-far ideal positive charge was determined to be TiO^{3+}, while the ideal negative ion was not yet tested fully, but early results showed TiO^- to be promising. In addition, plans to test cathodes with PbF_2 in the mixture to encourage the formation of fluorides have already been started before the beginning of this thesis.

With the previous experiment clearing the cathode material question, the next questions revolve around the optimal material, mixing ratio and yield thereof for di fferent molecules. In addition,

details about the chemical procedure must be answered once tests with commercial Ti powder conclude.

4.2. Negative ion yield

4.2.1. Yield

Initially, it is not clear which molecule on the low energy side of VERA should be used to deliver the Ti to the high energy side and thus the detector. Different molecules have vastly different efficiencies of forming in the ion source and must thus be checked individually. This is accomplished by measuring the yield.

To calculate the yield, the cumulative current in FCI 1-1 is compared to the total number of titanium atoms, in this case ^{48}Ti, in the respective cathode.

$$\text{Yield} = \sum_i \frac{I_i \cdot t_i}{N_{\text{Ti-48}} \cdot e} \tag{4.1}$$

Where in equation 4.1, I is the ion current measured each turn in the Faraday cup, t is the time over which it was measured. In practice, t is the average time calculated from all consecutive mass scans and I is the average current of each run. The total yield is the sum of all run-wise yields, signified by the index i. $N_{\text{Ti-48}}$ is the number of ^{48}Ti atoms in the cathodes and e is the unit charge. Typical yields are in the range of 0.1% to 3%.

Molecules that may form strongly at the beginning could decrease in current quickly which may be disadvantageous compared to another, more stable molecule. Considerations like sample material in the cathode, additional chemicals to encourage the formation of more complex molecules, unfortunate mass coincidences with abundant stable molecules that would falsify the yield and sufficient current must all be made.

Furthermore, a metal binder is added to discourage electrostatic charges to form in the sample material which would make the current less stable. It must be evaluated which mixture between titanium, in which ever compound, and said binder is most efficient at typical time scales of a beam time.

Note that the yield is highly dependent on the mixture in the cathode and typically only deviates one or two ‰ between individual cathodes. A experiment at VERA has shown the best yield to roughly be 1% for titanium fluorides, specifically TiF_3O^-.

This parameter is a very important metric for any new development at VERA. The higher the yield, the more material can be used in the measurement of any given sample. It can be understood as a form of 'efficiency' for a specific mixture. Before assessing yield, tests must be carried out to determine the ideal molecule of which to measure the yield.

To this end, a so called mass scan is carried out. This means that the field of the magnet in front of the cooler is increased by increasing the coil current starting at 35 A and going up to 165 A in most cases. At all current steps in the magnet, the ion current in FC I1-1 is recorded, resulting in a graph that shows how much ion current arrives at FC I1-1 at what magnetic field in BMI 1-1. Since a given magnetic field corresponds to a certain ionic mass, the final result ideally is a plot of ion current against ion mass.

To achieve this, a calibration is done between the coil current in the magnet and the corresponding mass. The ideal calibration curve is a 4th order polynomial which best describes the behavior of that part of the facility (see e.g. [34] for details).

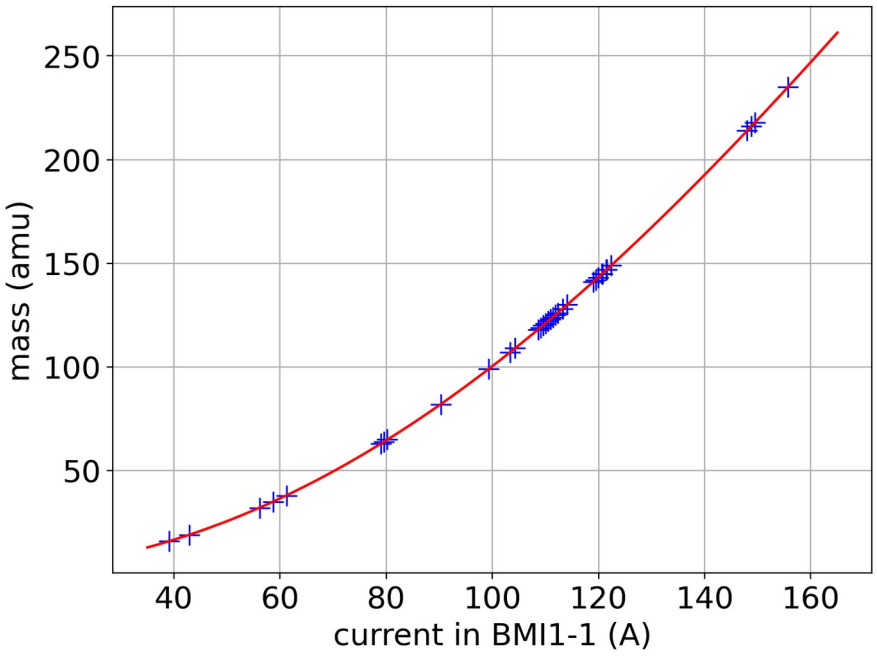

Figure 4.2.: A typical mass-current calibration curve. The x-axis shows the current in the first bending magnet in ampere and the y-axis is the mass in amu. The red line is the best fit through the calibration peaks that are signified as blue crosses.

Figure 4.2 shows the calibration curve that is used when identifying peaks. This is of course not necessary in every experiment, but is required to ensure reliable peak identification when testing yields with different molecules.

Experimental setup

The second ion source at VERA was utilized for all measurements due to its access to ILIAMS. Among the many source parameters, the most important ones are the line heater current (LNH), the cathode voltage (CAT), the extraction voltage (EXT), the ionizer current (ION), the oven voltage (OVN) and the voltage on the pre-accelerator (HVS).

Name	CAT	EXT	ION	OVN	LNH	HVS
Value	-4.601 kV	12.612 kV	125 W	32.015 V	18 A	-12.576 kV

Table 4.1.: The important source parameters, in this specific case from Ti2502, but should not deviate greatly from typical values. Note that the OVN temperature amounts to around 200°C.

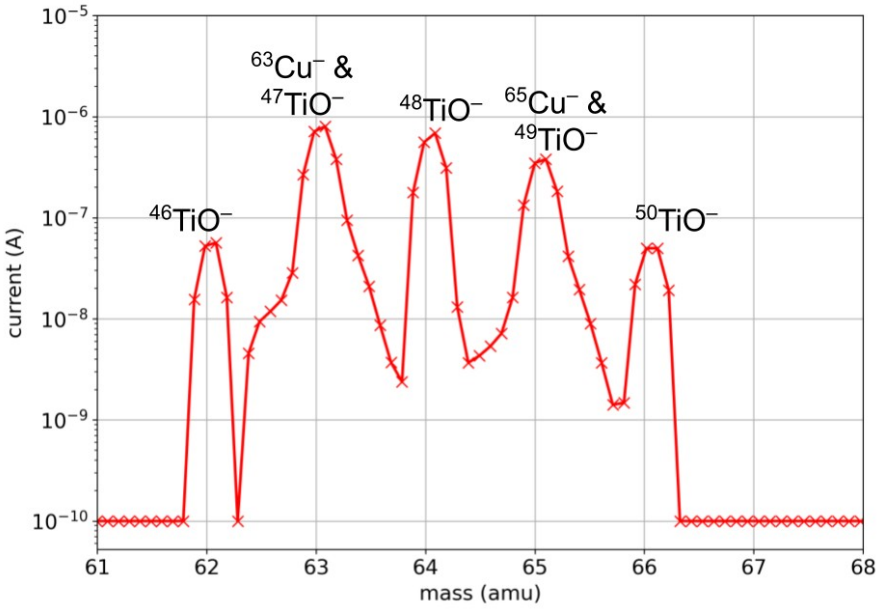

Figure 4.3.: A section of the mass scan centered around 64 amu. The x-axis shows the mass in amu while the y-axis shows the current of the ion beam. At mass 64 ^{48}TiO$^-$ can be seen. To the left of it are the peaks of ^{46}TiO$^-$ and ^{47}TiO$^-$, with ^{63}Cu$^-$ also at mass 63. The same is true for the right with ^{49}TiO$^-$, ^{50}TiO$^-$ and ^{65}Cu$^-$. The copper can be expected as the cathode itself is copper.

While the parameters cannot be identical between beam times, CAT and EXT were kept constant throughout all beam times. These values act as a rough guide to stand in place for the typical source parameters.

4.2.2. Assessing the ideal molecule

During the process of assessing the right ion for the beam, titanium oxides and titanium fluorides have been investigated in regards to their stability, overall yield and isobar suppression. While ultimately the oxides proved to be more promising, the progress with fluorides should not go unmentioned.

Fluoride tests

The Cu cathodes for these beam times were filled with a mixture of TiO_2:Ag:PbF_2 in a ratio of 1:1:9. Tests were also carried out with TiO_2:PbF_2 with a ratio of 1:9 but were dismissed due to unstable current during tuning and TiO_2:Ag:PbF_2 in 1:1:3 that were deemed non ideal due to low fluoride currents of $\lesssim$100 nA after the first bending magnet compared to usually more than 200 nA in later experiments.

All the currents have been measured in FC I1-1, as is usually the case for yield measurements at VERA.

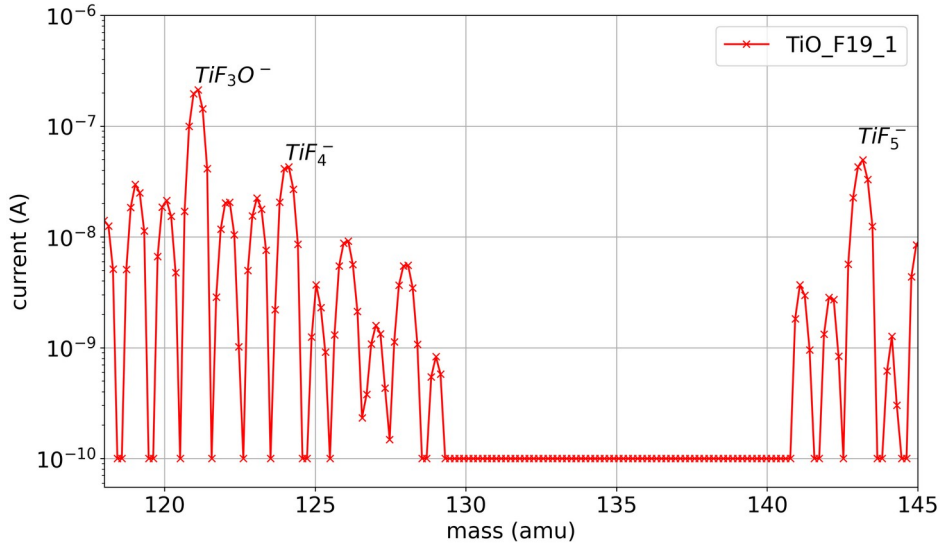

Figure 4.4.: The three most important fluoride peaks for the tests in a mass scan. The y-axis shows the recorded current while the x-axis shows the mass calibration, thus getting a spectrum of masses and their corresponding currents. Note that TiF_3O^- is higher by around a factor of 5 than TiF_4^- and TiF_5^-. Please also note that the structures around the marked peaks are characteristic for Ti, as the five stable isotopes form these kinds of peaks. ^{46}Ti and ^{47}Ti have an abundance of ≈8%, while ^{48}Ti has 75%, leaving 5% each for ^{49}Ti and ^{50}Ti.

Initially, multiple mass scans were carries out to ensure the reliable formation of a sufficient amount of fluorides. Many different fluoride molecules have been observed, including prominently TiF_3O^-, $TiF_4{}^-$ and $TiF_5{}^-$, among others. Following yield tests, the most promising molecules with the titanium fluorides were, in ascending order of yield, TiF^-, $TiF_4{}^-$, $TiF_5{}^-$, $TiFO^-$, TiO^-, $TiFO_2^-$ and TiF_3O^-.

Whilst initially promising, $TiF_4{}^-$ was dismissed as the current of this anion decreased consistently faster than the others. This would limit measurements of any given samples to only about an hour and would require more material per measurement in the cathode. Following tests with the cooler and the green and UV laser, the suppression of the isobar at mass 117 ($^{44}CaF_3O^-$) was almost non-existent, ruling out TiF_3O^- as well.

While the suppression of $CaF_5{}^-$ also only turned out to be a factor of 10-100, the isobar could still be partially distinguished from the isotope in the detector for the most part. Should other methods fail, this could present as a viable ion for further testing, provided that the separation would be maintained with actual ^{44}Ti.

ion mass (amu)	TiO^- 64	TiF^- 67	$TiFO^-$ 83	$TiFO_2^-$ 99	TiF_3O^- 121	TiF_4^- 124	TiF_5^- 143
1:1:9 TiO_2:Ag:PbF_2							
average yield (%)	0.27	0.05	0.19	0.34	0.94	0.10	0.19
standard deviation (%)	0.03	0.01	0.02	0.09	0.31	0.03	0.01
1:1:3 TiO_2:Ag:PbF_2							
average yield (%)	0.52	0.09	0.19	0.11	0.17	0.02	0.01
standard deviation (%)	0.10	0.02	0.02	0.01	0.02	0.01	0.01

Table 4.2.: Typical yields over various cathodes of the early beam times with fluorides for two 1:1:9 TiO_2:Ag:PbF_2 cathodes and two 1:1:3 cathodes with lower yield for everything but TiO_2. The uncertainties come from the scatter of different cathodes.

Table 4.2 shows the yields of early beam times with aforementioned Cu cathodes with TiO_2:Ag:PbF_2 in 1:1:9 and 1:1:3. Note the relatively high yield of TiF_3O^- with respect to the other fluorides in 1:1:9.

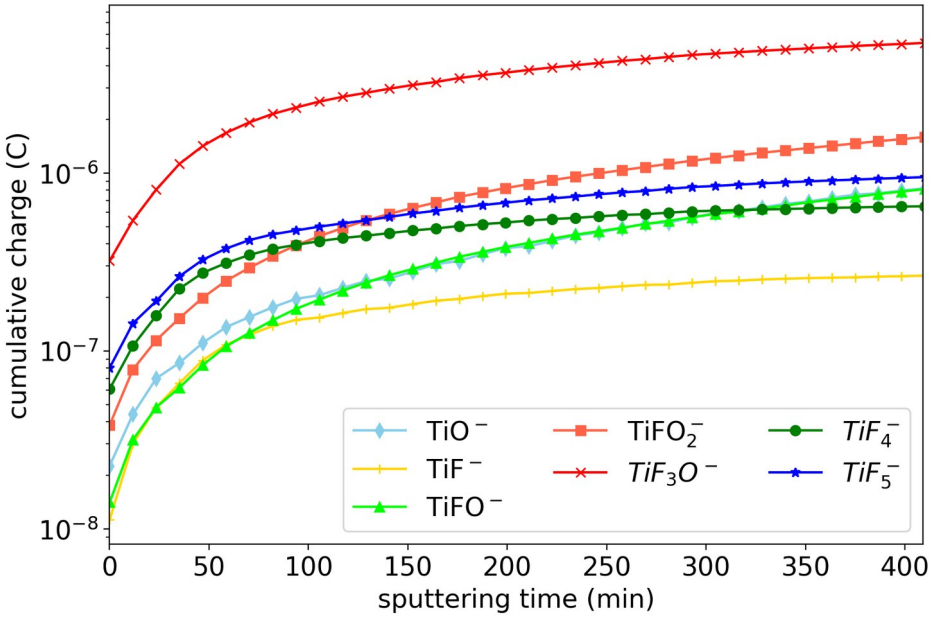

Figure 4.5.: The cumulative currents collected for different ion species extracted from of one cathodes with Ti:Ag:PbF_2 material in 1:1:9. The x-axis shows the sputter time in minutes and the y-axis is the cumulative charge in Coulomb. The various colors and markers each denote the current of one molecule.

Figure 4.5 shows the cumulative current of one cathode of all tested molecules in Ti2406. It is interesting to note that TiF^-, $TiFO^-$ and TiO^- start out very similarly but their trends end quite differently. It is also surprising that TiF_4^- has less overall current than TiF_5^-, despite the latter

needing more fluoride to form. It seems that TiF_5^- just forms better under the conditions in the ion source. These results agree with the fluoride findings in [35].

Finally a few notes on what not to do in the course of chemical sample preparation should not go unmentioned for future attempts. TiF_4 forms from Ti compounds and HF which was present in the ICP solution. Unfortunately, TiF_4 starts to decompose at ≈260°C, meaning that if fluorides are ever to be considered, calcination above 260°C is not an option. In addition a small amount of TiF_4 will have formed in the ^{44}Ti beam time given the 0.1% HF in the Ti ICP solution even when working with oxides.

To summarize, pure fluorides don't form efficiently, oxy-fluorides show a clear advantage in yield and in current. Unfortunately, none of the tested oxy-fluoride isobar molecules showed sufficient suppression with the tested lasers. From this, it can be concluded that currently, fluorides are presently not recommended for the measurement of ^{44}Ti at VERA using ILIAMS.

Oxide tests

Given the disadvantages of fluorides, oxides may provide the necessary suppression. In tests with the cooler and a borrowed optical parametric oscillator (OPO) laser, suppression has shown to be remarkable with TiO^- on the low energy side. Further, a relatively simple chemical preparation and the availability of commercial TiO_2 make oxides the prime candidate. All cathodes for this test were TiO_2:Ag (1:2). There are two types of cathodes, namely ones with roughly 2.5 mg of material and ones with 1 mg. The ion currents have been measured after the ILIAMS section of the accelerator in FC I1-1. Details to the cooler and laser tests can be found in section 4.3.1.

Without much prior experience, the ideal negative molecule must be evaluated by looking at the yield of several titanium oxides, namely TiO^-, TiO_2^- and TiO_3^-. Usually, the molecule with the least oxygen forms more efficiently. From figure 4.6, it is not difficult to choose the best molecule for further measurements. TiO^- shows the highest ion current consistently, at worst only equaling that of TiO_2^-. The only disadvantage of TiO^- is its steep drop after around an hour, where TiO_2^- stays more consistent.

The ideal molecule on the LE side can be concluded to be TiO^-. After the accelerator, one must pick the ideal positively charged state of Ti. To this end, currents have been measured on the HE side before the start of this project already, and Ti^{3+} turned out to be the best charge state at the relevant accelerator voltages.

In terms of actual yield, the three different oxide molecules result in (0.59±0.04)% for monoxides, (0.28±0.03)% for dioxides and (0.06±0.01)% for trioxides for the heavier 2.5 mg cathodes. It should be noted that after about four hours, the current of TiO^- and TiO_2^- are virtually the same. The lighter cathodes with 1 mg mass have slightly lower but comparable yields with (0.57±0.05)% for monoxides, (0.20±0.03)% for dioxides and (0.04±0.01)% for trioxides.

As figure 4.3 shows, the measured TiO^- peak is nested in between two prominent Cu peaks from masses 63 and 65 respectively. It was necessary to evaluate the influence of said peaks on the measured current at mass 64. To this end, Al_2O_3:Ag cathodes in a ratio of 1:1 have been pressed and sputtered for extensive amounts of time to spot potential contributions from tails of the neighboring peaks.

Figure 4.7 shows a cathode of TiO_2 to Ag in 1:2 at the very beginning of sputtering and at the very end, respectively. Note how the middle of three big peaks ($^{48}TiO_2$, see Figure 4.3) disappears

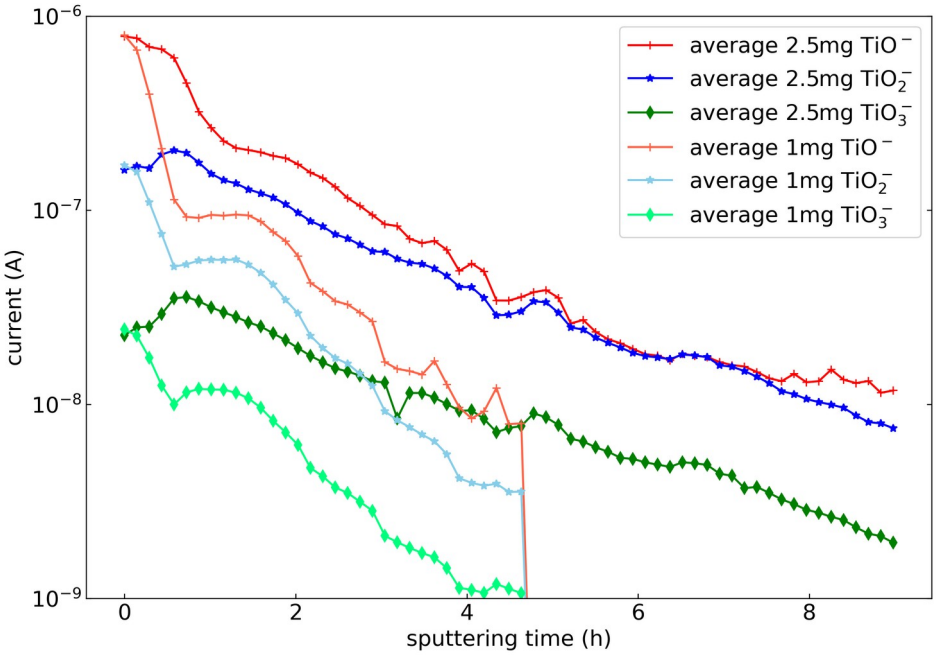

Figure 4.6.: The average current of various titanium oxide molecules from different cathodes on the y-axis against sputter time on the x-axis. Cathodes with more material perform better in terms of current over time and TiO^- is the molecule with the most optimal current trend over time. Note how after $\approx$4 hours, TiO^- and TiO_2^- perform very similarly. The material for both types of cathode was TiO_2:Ag(1:2). The 1 mg cathodes were taken out of the measurement due to low current at around four and a half hours.

over the course of the beam time where over the same time, the two adjacent copper peaks grow in current. The tail of the left copper peak reaches far enough into the $^{48}TiO_2$ peak to contribute to its current. Also note how the two small peaks of the isotopes ^{46}Ti and ^{50}Ti also disappear in the later turns.

As can be seen in figure 4.8, the overall contribution from tails of Cu are not negligible in the context of yield measurements. However, fortunately for the progress of this work, the contribution only becomes significant at around the three hour mark, thus exceeding typical measurement times.

When taking the cumulative current (the integral over the whole current), contributions from the non-Ti control cathodes are generally limited to $\lessapprox$1%. On average, the contribution of both of the non-Ti cathodes turn out to be 0.79% of the mean of the 2.5 mg TiO_2 cathodes.

It must be emphasized here that this is only the current on the low energy side, of course. No counts can be influenced from current by the Cu peaks to each side of mass 64. The worst thing that could happen is that our LE current measurement may be wrong by about 10% at the absolute worst after a few hours of sputtering.

To summarize, the most efficient molecule on the LE side appears to be TiO^-. While TiO_2^-

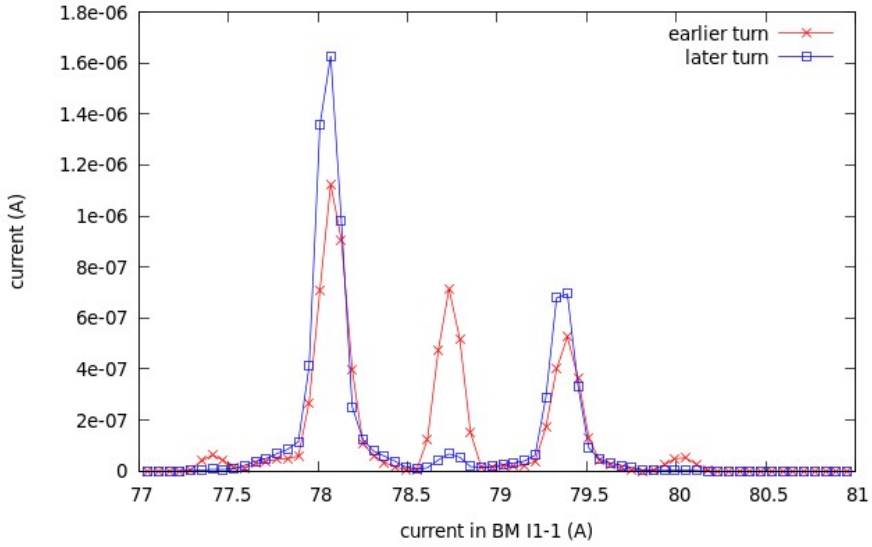

Figure 4.7.: A section of the mass scan centered around 64 amu. The x-axis shows the current in the first bending magnet while the y-axis shows the current of the ion beam itself. This is the same section as can be seen in Figure 4.3. The middle of the three higher peaks is the current that is measured for yield, $^{48}TiO^-$.

was more stable, the higher current and thus yield of TiO^- make it the better candidate.

4.2.3. The most efficient mixing ratio for TiO^-

In addition to finding a molecule that works in terms of suppression and yield, finding the correct mixing ratio with the metal binder is an additional task that needs to be analyzed. For this, three types of samples have been mixed and tested in terms of yield. The current has again been measured in FC I1-1.

Type	Mixing Ratio	planned sample weight (mg)
TiO_2_Ag_11	TiO_2:Ag in 1:1	1.67
TiO_2_Ag_12	TiO_2:Ag in 1:2	1.67 & 2.50
TiO_2_Ag_14	TiO_2:Ag in 1:4	1.67

Table 4.3.: The three different kinds of cathode for the yield tests.

Table 4.3 shows the different mixing ratios for the yield efficiency tests. Note that there are three cathodes each for types 11 and 14, and 6 for type 12 to test for potential differences in total mixture mass. Note that the actual weightings can be found in table A.1.

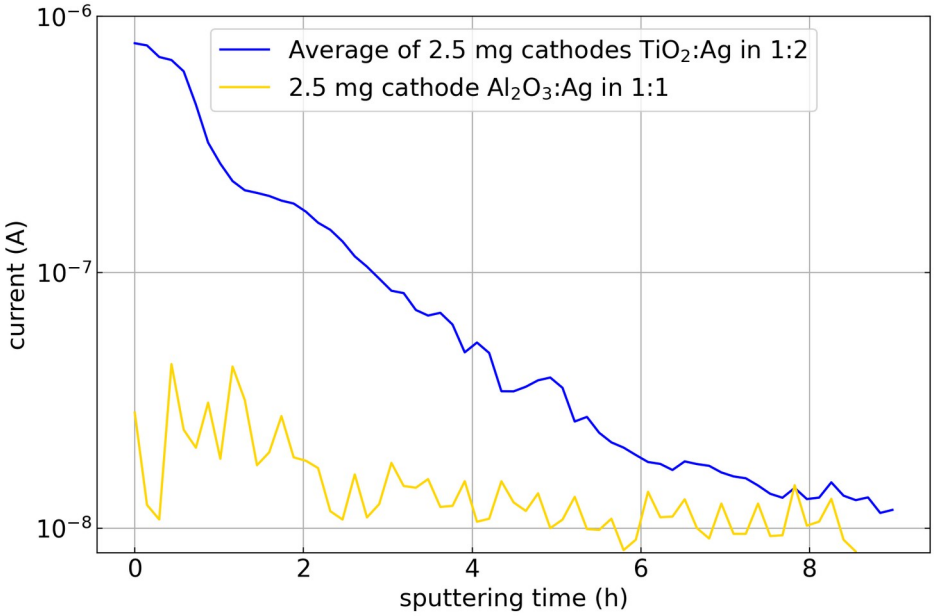

Figure 4.8.: The contribution of non-Ti cathodes to current at mass 64. The y-axis shows the current at mass 64 where TiO^- would be, and the x-axis shows the sputter time. The blue graph shows the average over all 2.5 mg TiO_2:Ag cathodes in that beam time and the yellow graph shows the current from the single Al_2O_3:Ag cathode.

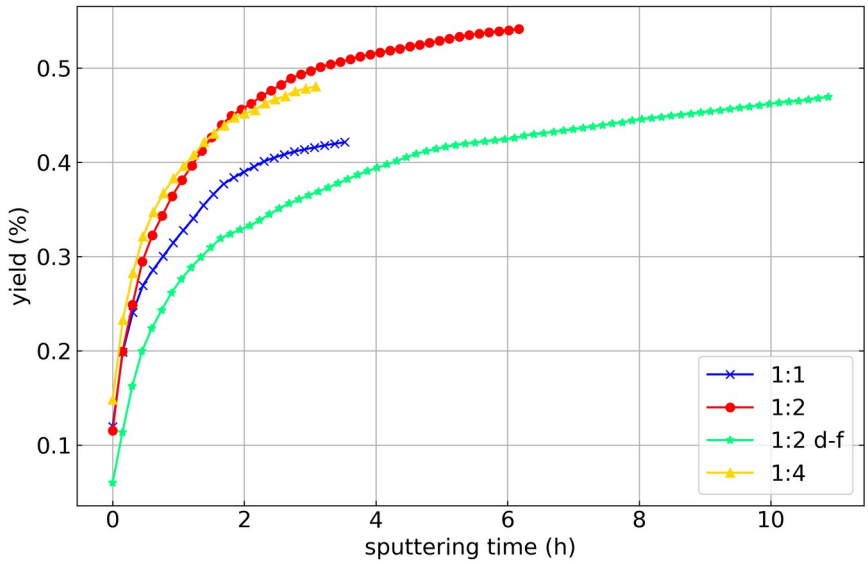

Figure 4.9.: Cumulative yield vs. measurement time of various mixing ratios of TiO_2:Ag. The x-axis shows the sputter time in hours and the y-axis shows the cumulative, negative ion yield of TiO^- in %. The various markers show different mixing ratios, with the green markers showing the mixing ratio 1:2 d-f that have more cathode material, 2.50 mg instead of 1.67 mg. See tables 4.3 and A.1 for details. From this, both 1:2 and 1:4 seem reasonable ratios for further measurements.

As shown in figure 4.9, the total yield of TiO^- does not exceed 0.6%. That is a good bit above what was expected from earlier beam times with fluorides that have been closer to 0.3% for TiO^-. This may be due to inconsistent yield results or come from the lower overall amount of Ti in the cathodes used for fluorides.

Interestingly, there is little difference between the ratio 1:4 (yellow markers) and 1:2 (red), as they show similar cumulative yields over the measured time. It should be noted here that typical measurement times are unlikely to reach four hours, so for all practical purposes it can be said that 1:2 and 1:4 behave similarly. Later beam times confirmed yields around 0.6% with a 1:2 ratio.

It must be noted here that yield is not the only consideration when choosing the ideal mixing ratio. Ratios with a higher amount of Ag for stabilization of the current can be beneficial if the sample material is scarce. Conversely, if sample material is abundant, a lower ratio may be chosen to receive higher currents, particularly in the beginning of the measurement.

In this case, 1:2 was chosen for follow up tests and measurements as it consistently delivered the more stable current and a stronger starting current, which proved beneficial for tuning the facility.

As can also be seen in figure 4.9, Ti cathodes last for a surprisingly long time given the little material in them compared to most others. As typical measurement times are unlikely to exceed three hours per cathode, as little as 1-1.5 mg cathode material may already be enough for most purposes. Additionally, the yields were lower for cathodes with more material in them, but of course lasted longer.

4.3. Isobar suppression methods

Since ^{44}Ca is stable and Ca is abundant in many everyday things such as sweat, glass and can even be found in dust, a way of suppressing the contributions from it must be found. This suppression is achieved by utilizing differences in electron affinities. Table 4.4 show literature values for relevant electron affinities. Ideally, a laser would be available that is in between 0.8 eV and 1.2 eV. No lasers were suitable at the time of testing, but luckily a tuneable laser was borrowed by VERA from the University of Mainz for experiments using ILIAMS.

Molecule	Electron Affinity (eV)	Method
CaO	0.7	Measurement [36]
CaO	≈0.8	Simulation [37]
TiO	1.3	Measurement [38]
TiO	1.2-1.4	Theory [39]

Table 4.4.: Literature values for electron affinities. Note that the electron affinity is usually evaluated for the neutral molecule. As is evident, there is a difference in electron affinities that could be sufficient for effective suppression of CaO.

It must be emphasized here that no exact mechanism for either the cooler gas interactions, or the laser interaction are known. As noted before, CaO poisons the ionizer, so testing for molecular

break-ups after the cooler was not easily possible within the context of this thesis as it requires macroscopic ion beams. It is not known if the OPO laser broke up the whole molecule or merely detached an electron. The same holds true for the gas interactions. ILIAMS and its parts can be seen more detailed in figure 2.3.

4.3.1. Lasers

Due to the visit from the Johannes Gutenberg-Universität Mainz, tests were conducted with an OPO laser on titanium oxide samples, as the believed detachment energy for TiO is around 1.2 eV to 1.4 eV and for CaO as low as 0.8 eV to 0.7 eV (see Table 4.4) which is within the normal operating range of the specific OPO. For an overview of the lasers that are available for ILIAMS, see section 2.1.1.

For testing, four samples were prepared of two mixtures each. Both mixtures contain TiO_2 and Ag in a ratio of 1:2 and one contains 0.1 parts of CaO_2 in addition. Ca was added to explicitly test its suppression. Two experiments were conducted with the mixtures, once testing with the OPO laser, and testing with various cooler pressures not carried out at earlier attempts with titanium oxides. For details of the samples used in the tests with the TiSa laser, see section A.1.2.

More specifically, the facility was tuned to the first FC after the accelerator (FC 03-1) for measurements of stable $^{48}Ti^{3+}$ current, and to the detector for measurements of Ca $^{3+}$ counts. Several tests were carried out, with the laser either turned on or off, measuring the currents or counts, respectively.

λ (nm)	energy (eV)	Ti^{3+} (nA), off	Ti^{3+} (nA), on	power (mW)	suppression
1100	1.13	92	54	640	1.70
1200	1.03	87	78	570	1.12
1300	0.98	87	81	550	1.07
1325	0.96	54	52	530	1.04
1350	0.94	53	53	510	1.00
1400	0.92	87	87	450	1.00
1500	0.83	100	100	430	1.00

Table 4.5.: The measured high energy current of Ti^{3+} with the OPO laser on and off at various photon energies between 0.83 and 1.13 eV including the laser power and the suppression factor calculated as the ratio between laser off vs. laser on. Note that the given laser power was measured after the cooler.

From tables 4.5 and 4.6 it can be seen that around 0.94 eV there is an area where almost all of the Ca^{3+} is being suppressed but Ti^{3+} remains almost untouched by the laser. This is the photon energy range in which a measurement of ^{44}Ti can be done reliably.

A second visit from the aforementioned guests from the University of Mainz together with their titanium-sapphire laser was the cause for follow up tests with it, as the one at VERA would only be installed later. During the tests, an energy area of roughly 1.36 eV to 1.45 eV (790 nm to 910 nm) was scanned to assess the trend of the stable TiO^- current in that region. As can be expected, this region shows a strong decrease in stable current relative to the lower energy region

energy (eV)	approx. Ca^{3+} cps (s^{-1}) laser off	Ca^{3+} counts in 60 seconds laser on	laser power (mW)
1.03	3000	0	500
0.98	3000	0	470
0.96	3000	2	530
0.92	3000	93	470
0.88	3000	3000	310
0.83	3000	3000	390

Table 4.6.: The measured counts in 60 seconds of Ca^{3+} with the OPO laser on and off at various energies between 0.83 and 1.03 eV.

below ≈1.1 eV. It must be emphasized here that the current during the second visit was higher due to the improvements made in between and that the currents can thus not be compared directly. Instead, we have chosen to scale the data in the following figure.

The important message must be that while there is some Ti current at the higher energies, the ideal energy for measurements is still in the lower energy region below 1 eV. To achieve the best possible TiO^- current, the lowest possible energy where CaO^- is still suppressed.
As can be seen in figure 4.10, the region surrounding 0.96 eV (≈1325 nm) has the ideal properties for future measurements as the isobar CaO^- is strongly suppressed while TiO^- is hardly influenced at only between ≲1% to ≈7% loss in the cooler at those energies.

Unfortunately, the OPO laser is not a permanent installation for ILIAMS and was only provided for exploration of its capabilities at the facility. However, it should still be considered a valuable insight into potential future projects with ^{44}Ti. Should the analysis of ^{44}Ti continue, an OPO laser or any other laser that reaches these energies is absolutely necessary. Without an additional laser, the background level of ^{44}Ti can likely only be improved in minor ways above the final result of this thesis. It must be noted that the brief test period with the OPO laser does not overlap with the later tests of ^{44}Ti samples. All results from there do not include any suppression with the OPO laser and only utilize cooler gas suppression.

Also note how the photon energy of roughly 0.9 eV is a little above the electron affinity listed in table 4.4. This could be due to a significant difference in electron affinity between CaO and the vertical detachment energy of CaO^-, but is otherwise a contradiction to the sources listen in table 4.4. Furthermore, the apparent influence of the laser at roughly 1.4 eV (around 830 nm) on the current of TiO^- occurs at energies that can be expected from the same table. Details on the TiSa in absolute numbers can be found in table A.3.

4.3.2. Cooler pressure variations

With the promising results for the OPO laser in place, the capabilities of the ion cooler without the laser and just with the cooler has must still be evaluated. To this end, experiments with varying cooler gas pressure have also been carried out. Both CaO^- and TiO^- beams were guided through the ion cooler at various He pressures between 3 Pa and 5.8 Pa (for a conversion between the displayed mbar scale on the device and Pa see [40]).

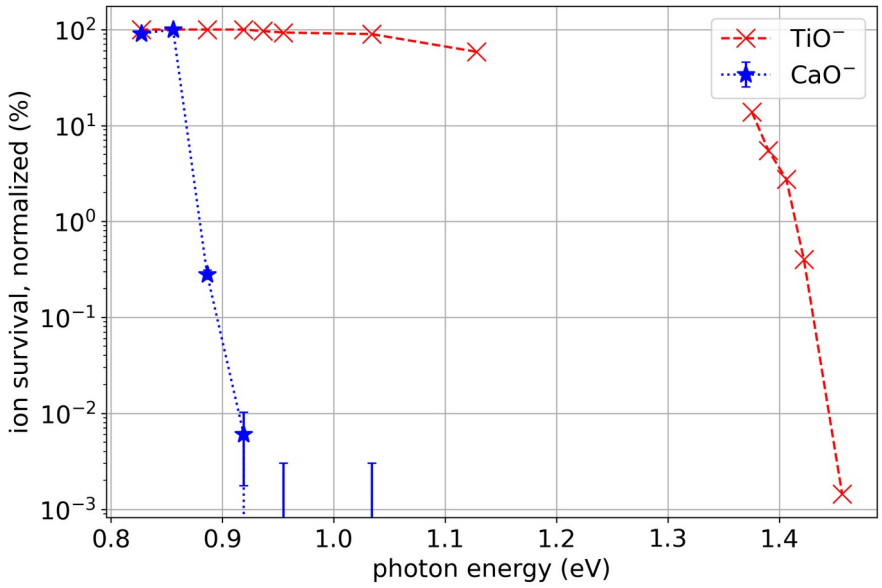

Figure 4.10.: The influence of the lasers, the OPO for the left group of data points and the TiSa for the right group of data points, on the two di fferent molecules. The y-axis is the ion survival fraction and the x-axis are the photon energies in eV of the OPO laser. The photon energies close to 0.96 eV (≈1325 nm) show the best suppression of the isobar while barely influencing TiO $^-$ currents making it ideal for future measurements with the OPO laser. Please note that the points for TiO $^-$ have been taken from two experiments at VERA that have been carried out with the and have been scaled to fit into one figure.

Table 4.7 shows the substantial decrease in counts per second of Ca^{3+} in the detector towards higher cooler pressures. As can be seen, the TiO $^-$ current in FCI 2-2 drops by less than 50% in the same range where Ca^{3+} drops by > 10^6.

The data of table 4.7 is visualized in figure 4.11. As noted earlier, the drop in intensity of the isobar of > 10^6 can be seen nicely in figure 4.11. The cooler thus improves the measurement by significantly suppressing Ca at high cooler gas pressures and should be used in all following measurements if possible.

Increasing the injector ion energy

By increasing the energy of the particles directly from the source and thus increasing the collisional cross section of the incoming molecules with the ion cooler gas, the additional energy may aid in dissociation of the molecules in the He gas of the ion cooler. To test this the energy of the ions was increased by roughly 20 eV after the fourth measurement turn of the final beam time. Even though Ca will decrease, it was unclear whether Ti would also decrease as strongly, possibly yielding no overall change in the end.

After impromptu tests during the ^{44}Ti beam time, it became evident that the additional energy

He pressure (Pa)	$^{44}Ca^{3+}$ cps (s^{-1})	TiO^- current (nA)
3.0	$\approx 6.5 \cdot 10^6$	2.75
3.4	$\approx 1.0 \cdot 10^6$	2.65
3.8	$\approx 7.0 \cdot 10^4$	2.51
4.2	$\approx 2.5 \cdot 10^4$	2.40
4.5	$\approx 4.0 \cdot 10^3$	2.23
5.0	500	2.05
5.4	20	1.88
5.8	3	1.77

Table 4.7.: The counts per second of Ca^{3+} and the current of TiO^- with various cooler pressures with He as buffer gas.

into the cooler had no clear effect on the overall ratios of the blanks. All samples showed lower currents and lower counts, the spikes more so than the others. Weighing the decrease in current and counts against the beneficial effects, no additional suppression factor can be gained this way.

Summary of isobar suppression

The OPO laser at roughly 0.96 eV (1325 nm) managed to suppress the isobar CaO^- by $\approx 10^5$, the gas interactions in the ion cooler with He pressure of 5.8 Pa by an additional $> 10^6$. This suppression allows an optimistic outlook, particularly if applied at the same time in future measurements.

4.3.3. Estimations of detector separation

Since actual ^{44}Ti was not available until the end of the project, early conclusions for the separation between $^{44}Ti^{3+}$ and $^{44}Ca^{3+}$ in the detector had to be drawn from measurement extrapolation. By recording the energy loss spectra of $^{50}Ti^{3+}$, $^{48}Ti^{3+}$ and $^{46}Ti^{3+}$ in the detector, the average distance between two isotopes of Ti could be estimated for a step of 2 amu.

The center of mass for each of the distributions were recorded and are depicted in the right panel in figure 4.12. Note that the distances between the two isotope pairs are not equal. For this reason, the average of the two distances was chosen to extrapolate to $^{44}Ti^{3+}$.

The separation seen in figure 4.12 between the Ti isotopes makes an estimate of the center of mass for $^{44}Ti^{3+}$ possible. The likely position was gotten by taking both distances between the measured Ti isotopes and taking the mean change in each direction. Afterwards, that distance was added to the $^{46}Ti^{3+}$ position to come up with the estimated $^{44}Ti^{3+}$ center of mass. To also account for the spread of the estimated $^{44}Ti^{3+}$ counts, the spread of $^{46}Ti^{3+}$ events is laid over the center of mass of $^{44}Ti^{3+}$.

As can be deduced from figure 4.12, the center of mass for $^{44}Ti^{3+}$ can be expected to the lower right side of the center of mass of $^{44}Ca^{3+}$ by what may be enough to distinguish between it and $^{44}Ti^{3+}$.

Figure 4.13 shows nicely that despite a substantial overlap, the two ion species have a good chance to be sufficiently distinguishable with a smart selection of regions of interest such that

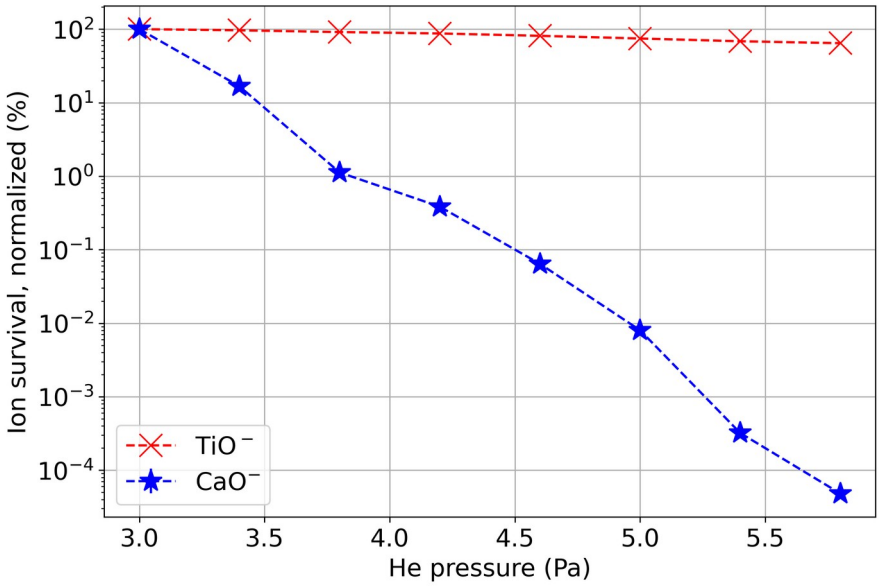

Figure 4.11.: The relative intensity of TiO$^-$ through the ion cooler in red and the relative intensity of CaO$^-$ in blue. As a function of the He pressure in the cooler in Pa. CaO$^-$ diminish by $\geq 10^6$ where TiO$^-$ current only decreases by a factor of 2. Note that, as can be seen in table 4.7, Ca was measured as counts in the detector where Ti was measured as stable current.

very few $^{44}Ca^{3+}$ counts may remain. Already from a very basic straight cut, around 95% of the $^{44}Ca^{3+}$ may be dismissed while keeping 95% of the $^{44}Ti^{3+}$, adding another hypothetical factor 20 to the Ca-suppression.

In principle, nothing prevents one from doing so even more drastically, possibly eliminating >99% of the $^{44}Ca^{3+}$ counts whilst retaining ≈30% of the $^{44}Ti^{3+}$ ones, allowing for an ever higher suppression of the isobar, but not exceeding a factor of 30. In practice, only about $^{44}Ca^{3+}$ counts contribute to the $^{44}Ti^{3+}$ counts with even moderate cuts like the one shown in figure 4.13.

All of the above estimations come from a linear separation between the two spectra in the detector, which is by no means the only method to be tried.

In the end, the best method for detector separation turned out to be the inbuilt method in VERA itself. Essentially, many cuts are drawn around the region of interest to exclude any tails, outliers and in the case of this thesis to optimize towards the sensitivity. A typical spectrum with true ^{44}Ti can be seen in Figure 7.4.

In summary, the yield of the ideal molecule, in this case TiO$^-$ has been established to be roughly 0.6% at a mixing ratio of either 1:2 or 1:4 with Ag powder. Fluorides have been largely discarded after either unfavorable current stability or a lack of isobar suppression. The ion cooler can suppress the isobar for oxides very well, by roughly a factor of 10^5 for interactions with He gas at ≈6 Pa and by a further 10^6 with a laser at 0.96 eV (1325 nm). The separation in the detector may allow for more than an additional factor of 30 to the suppression if the regions of interest are

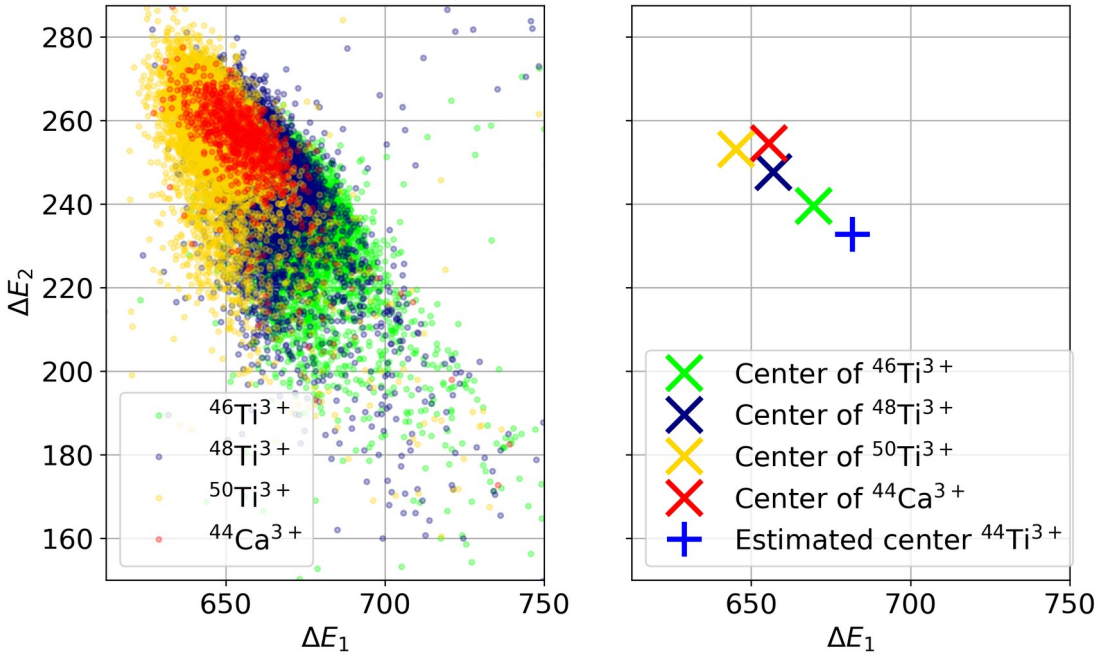

Figure 4.12.: The left panel shows the counts in the detector from $^{46}Ti^{3+}$ in green, $^{48}Ti^{3+}$ in dark blue, $^{50}Ti^{3+}$ in yellow and $^{44}Ca^{3+}$ in red. The right panel shows the corresponding centers of mass for each isotope in the same color and the estimated center for $^{44}Ti^{3+}$ in a lighter blue. As can be seen from the progression from $^{46}Ti^{3+}$ to $^{50}Ti^{3+}$, the expected center of mass for $^{44}Ti^{3+}$ is relatively far away from $^{44}Ca^{3+}$, possibly allowing for separation by choosing a suitable region of interest in the spectra.

cut in an optimal way. All pieces are in place to establish a chemical preparation procedure now that the ideal mixing ratio is established.

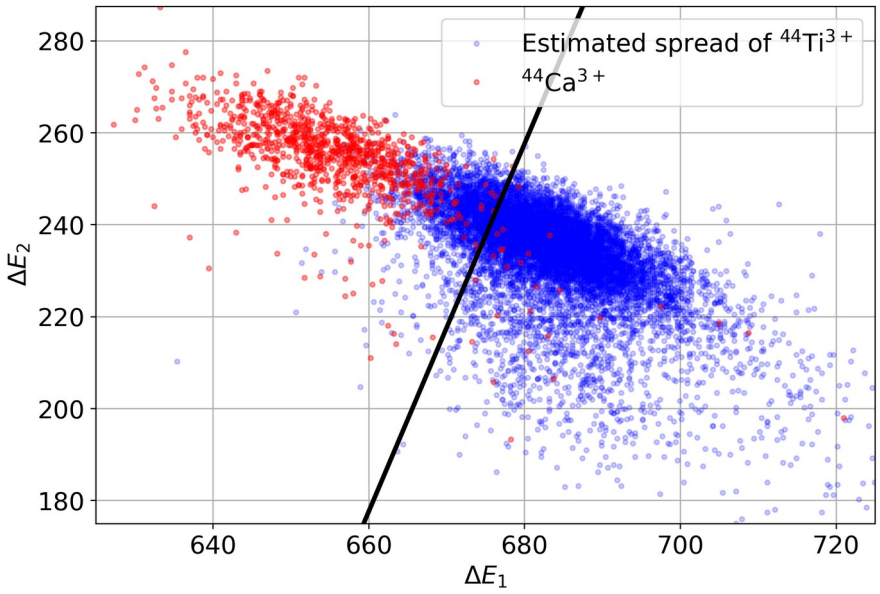

Figure 4.13.: Estimated spread of $^{44}Ti^{3+}$ events in the detector in blue and the measured spectra of $^{44}Ca^{3+}$ in red. The y-, and x-axis in this figure show energy loss on the first anode and on the second anode in channels of the detector. Note the clear separation between the centers of these distributions, possibly allowing for an additional factor of $\gtrapprox 20$ in terms of isobar suppression if a cut similar to the black line is implemented.

5. Chemical Sample Preparation

5.1. General preparation

Due to the lack of a commercially available ^{44}Ti standard, a self made in house standard needs to be produced. In this situation, it is the most lucrative and efficient method to buy or otherwise organize a known activity of ^{44}Ti, ideally liquid and dissolved in an acid, and add a known amount of stable titanium ourselves. The known amount of stable titanium stems from a certified solution from the company “Carl Roth”, that is described in more detail later.

The ideal result of this chemistry process is a TiO_2 powder, as per chapter 4, that can easily be pressed into the copper cathodes at VERA in amounts that range somewhere in the mg, such that a sufficient sputtering time can be achieved for any following measurements.

AMS test targets could be made from either powder or liquid. Since working with a liquid is more controllable due to precise instruments for dispensing small amounts down to µl and the ability for fluids to mix completely, it is the preferred way to produce samples in this project. With a powder, achieving exact mixing ratios is nearly impossible and even thorough mixing does not guarantee uniform distribution when pressed into the cathode. Thus, working with solutions is more precise. Note that most standard solutions are also in liquid form, as is true for the Ti Inductively Coupled Plasma (ICP)[1] standard solution that was used for all standards and some tests, while samples made for general tests with VERA, i.e. yield, suppression, and early detector spectra were made from commercial TiO_2 powder for ease of use.

In general, the way to turn the Ti solution into a powder is to precipitate it as $Ti(OH)_4$, to wash this precipitate and ignite it in a muffle furnace at high temperatures to create TiO_2.

Weighing

In order to conduct later yield tests, the cathode and pin with the material weight must be known very precisely. The scale in the weighing room can measure as precisely as 0.01 mg, for high accuracy measurements due to influences from electrostatic effects, an uncertainty of 0.05 mg is assumed, and prior to yield test, every cathode together with it’s later pressing pin was weighed and stored separately. After the sample material was added, the whole assembled cathode was weighed again. Typically, between 1.5 mg and 3 mg were used for tests with TiO mixtures.

[1] Refers to the method with which the analysis technique that was used to determine the elemental composition, in full Inductively Coupled Plasma - Optical Emission Spectroscopy.

5.2. Handling & pressing

^{44}Ti inhouse standards

All the standards have been prepared from (12.05±0.25) kBq activity of ^{44}Ti, kindly sent to us by the PSI in late February 2025. The activity came in a 2% HNO_3 solution. At first, the activity was diluted in (26.25200 ±0.00005) g of stable Ti ICP carrier solution (company "Carl Roth", lot 909008)[2] with a concentration of stable Ti of (9484±28) $\mu g/g_{solution}$. This yields a first solution with a ratio $(1.032 \pm 0.020) \cdot 10^{-8}$ of ^{44}Ti to stable Ti. The uncertainty stems from the weighing uncertainties, from the solution uncertainty and from the uncertainty of the activity. This solution is our master solution for all further dilution steps and is labeled as SMV-Ti-08. Only about 1 mL of it was used, making almost 25 mL available for follow up measurements from the same base solution.

As the total amount of Ti per dilution is around 20 mg in each standard, the blank was prepared with the same amount (≈20 mg). For this, (2.04871±0.00007) g of the Ti ICP solution are treated in the same manner as the standards.

In order to evaluate the accuracy and any potential issues arising during the measurement, AMS standards need to be produced. An AMS standard has a known ratio between the radionuclides and its stable counterparts. If this standard has been measured at several other facilities previously in a round-robin exercise or is prepared by a metrology institute using primary methods, it is a "primary standard". It must be noted here that there is no widely used or accepted primary standard available for ^{44}Ti as there has been no AMS measurements of it in many years.

For each standard, the rough goal for total Ti in the end was 20 mg in order to have plenty of material left for further beamtimes, calculating at most 2 mg of Ti per cathode, which corresponds to about 2 g of the ICP solution out of which the standards mainly consist. From this, the amount necessary of the previous dilution to reach the desired ratio can be calculated. After an aliquot from the previous dilution is taken and further diluted with the Ti ICP solution, it is put aside to equilibrate for about a day in a 5 mL eppi. When this is done, the dilution is briefly centrifuged to get any stray droplets from the walls back in with the rest.

The consecutive steps after the SMV-Ti-08 standard has been prepared can be seen in table 5.1.

Name	Aliquot prior solution (g)	Ti ICP solution (g)	Total stable Ti (atoms)
SMV-Ti-09	0.979 00 ± 0.000 05	1.049 00 ± 0.000 05	$(2.42 \pm 0.01) \cdot 10^{20}$
SMV-Ti-10	0.202 24 ± 0.000 05	1.799 95 ± 0.000 05	$(2.39 \pm 0.01) \cdot 10^{20}$
SMV-Ti-11	0.198 88 ± 0.000 05	1.795 44 ± 0.000 05	$(2.38 \pm 0.01) \cdot 10^{20}$
SMV-Ti-12	0.198 58 ± 0.000 05	1.786 63 ± 0.000 05	$(2.37 \pm 0.01) \cdot 10^{20}$

Table 5.1.: The listing of what was taken from each solution to prepare the next dilution step. The left column shows how much material from the prior solution was taken to create the "current" solution. The second column indicates the amount of the Ti ICP solution that was used for each step. The rightmost column is the resulting amount of stable Ti atoms. The stable Ti concentration is always close to 9480 µg/g

[2] the VERA internal marking is bottle 905

The uncertainties in the right column in table 5.1 stem from the initial activity uncertainty from the material from the PSI, as well as the weighing uncertainty from the scale. As is evident, the uncertainty from weighing is well below the ≈2% of the activity, thus hardly contributes. All details about the chemistry can be found in section A.1.3.

In table 5.2, all the important data about the samples used to establish the detection limit can be found. The processing blank ideally has no ^{44}Ti in it.

Name	nominal ratio ^{44}Ti/Ti	^{44}Ti (atoms)	Activity ^{44}Ti (Bq)
SMV-Ti-09	$(4.970 \pm 0.094) \cdot 10^{-9}$	$(1.08 \pm 0.03) \cdot 10^{12}$	$(4.03 \pm 0.09) \cdot 10^{2}$
SMV-Ti-10	$(5.012 \pm 0.095) \cdot 10^{-10}$	$(1.08 \pm 0.03) \cdot 10^{11}$	$(4.03 \pm 0.09) \cdot 10^{1}$
SMV-Ti-11	$(4.998 \pm 0.094) \cdot 10^{-11}$	$(1.07 \pm 0.03) \cdot 10^{10}$	$(4.00 \pm 0.09) \cdot 10^{0}$
SMV-Ti-12	$(4.999 \pm 0.095) \cdot 10^{-12}$	$(1.18 \pm 0.03) \cdot 10^{9}$	$(4.40 \pm 0.10) \cdot 10^{-1}$

Table 5.2.: Nominal values for the standard dilution series. The first dilution, SMV-Ti-08, is not listed as it was not converted to TiO_2. Please note that the activity of ^{44}Ti was not measured but was calculated from the weighed amount of solution during the creation of the dilution series. Note that the given numbers are in total for the whole standard material.

Note that the names of all the standards, SMV-Ti-XX is composed of the responsible chemist, Silke Merchel and was prepared in Vienna. Ti of course stands for titanium and the two numbers indicate the order of magnitude of ^{44}Ti/stable Ti. The ratios have been determined by blank measurements from both commercial TiO_2 and in house produces ones from Ti-ICP solution. The tests of those blank measurements can be seen in chapter 6.

In order to produce TiO_2, a precipitation with NH_{3aq} needs to be carried out with $Ti(OH)_4$ as an intermediate step. To this end, drops of 25% NH_3 are added to SMV-Ti-X solutions until the pH reaches ≈9-10 which is measured with pH test strips. When the solution has the correct pH value a white, cloudy precipitate instantly forms. The solution rests for a minimum of a few hours such that the precipitate can age to prevent it from redissolving in further handling.

After this step, the material in the 5 ml vial is centrifuged at 4000 rpm for 5 min separating $Ti(OH)_4$ from the supernatant, which ideally contains very little Ti. The centrifugate is decanted. The precipitate is now washed with deionized water three times to remove all ammonia and anions like NO_3^{2-} and F^- (from the dilute acid from the ICP and the PSI solution) still present as it would form other solids like NH_4NO_3, which can hinder the AMS measurement.

Following the washing step the hydroxides are transferred into a previously weighed quartz crucible with a quartz holder/cap. The crucible is then put covered by a beaker with a hole in it onto a hot plate at 90°C for several hours until dry. To get rid of any remaining potentially salts that may be still present, the hotplate is turned to 400°C for around 15 min. After the crucible is cool enough to handle again, it is put into a muffle furnace at 900°C for two hours, and allowed to cool off afterwards. In the muffle furnace, the $Ti(OH)_4$ transforms to TiO_2. When the crucible has cooled off, it is sealed with parafilm with its cap and is stored to be mixed with silver powder and pressed into cathodes at a later point. A picture of the unsealed crucible can be seen in figure

5.1. The silver powder used for all samples is -120 mesh from Premion with 99.999% purity[3].

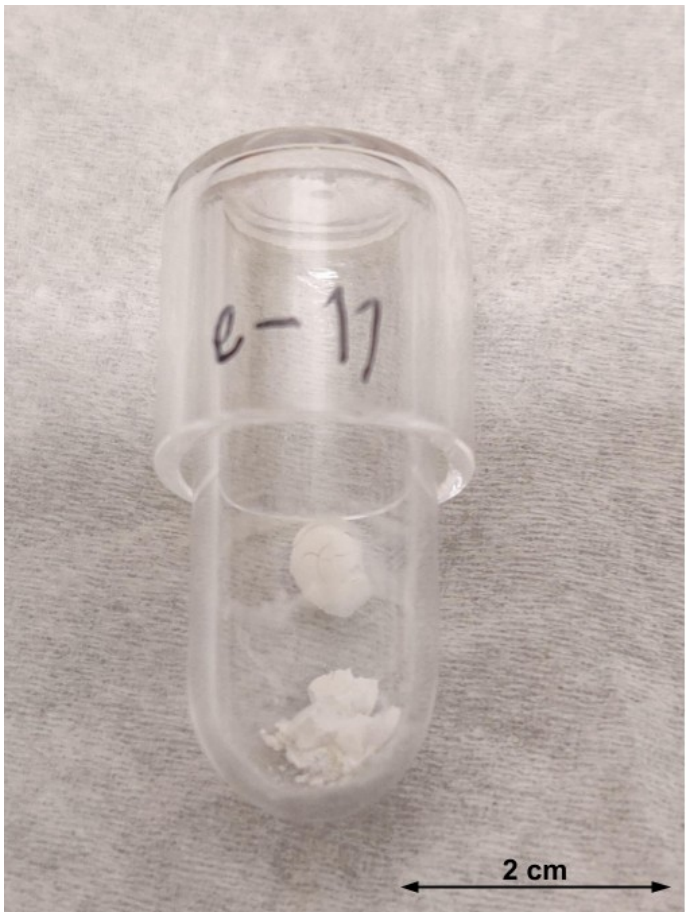

Figure 5.1.: White TiO2 powder (30 mg of SMV-Ti-11) in a quartz crucible covered with a quartz cap.

When preparing for pressing the cathodes, it is important to note that the white powder that can also be seen in figure 5.1 can be very brittle and hard to crush. Attention must be paid to the varying consistency of the material. All standards were easy to crush and turned into powder, but the blank material showed remarkable stability, requiring a lot of pressure and manipulation.

Fortunately, this was only the case for the blank and none of the samples containing ^{44}Ti showed this behavior.

Overall, chemical sample preparation seemingly worked well. The broad plan of $Ti(OH)_4$ precipitation, washing and ignition in the muffle furnace were tried and tested for relatively clean Ti samples. However, the chemical preparation of standards was easily possible since the ^{44}Ti from the PSI was made from vanadium. The same easy chemistry can be expected to be successful for the irradiated Ca samples as Ca does not for any precipitate at higher pH levels.

[3] the VERA internal marking is bottle 576

5.3. Potential sources of Ca contamination

Given that Ca is a common element of most everyday objects, it is no surprise that it can be found even in blank cathodes that were handled with great care. The first and likely largest source of Ca contamination is contact with human skin. Given that Ca is instrumental in normal body function aside from bones, some of it will have made it into the samples despite wearing gloves and taking care not to touch instruments and material. It is known that calcium in sweat can amount to 3 mg/dL [41]. One mL of sweat would already amount to $\approx 3 \cdot 10^{17}$ Ca atoms, of which 2%, close to $6 \cdot 10^{15}$, are ^{44}Ca atoms.

One additional suspected source of Ca surface contamination is the steel of the sample preparation tool and the pressing equipment (funnel, pressing pins,. . .). Steel can contain small concentrations of Ca in the order of 0.005%. Naturally, some of that steel will make it into the samples during handling.

Ca is also present in substantial amounts in dust, making the open handling of Ti samples by itself a source of contamination in normal surroundings. Depending on the source of the dust, Ca can even be the most abundant element present, but usually makes up ≈7% in weight [42]. A few micrograms of dust would already amount to several 10^{17} ^{44}Ca atoms. Only a dust-free lab or some sort of clean room would reduce this contribution.

With a reliable and reproducible chemical preparation established, an assessment of isobar suppression must be made in order to gain a realistic understanding for the later standards and any potential irradiated samples. Even blanks may suffer from Ca contamination due to the reasons listed and a solid suppression is instrumental in conducting a reliable measurement.

6. Blank Measurements

With the knowledge of the ideal mixing ratios and materials, it is necessary to measure what the background level, also known as the blank level is in order to create standards from those results.

For the preliminary "blank" measurements outside of the ^{44}Ti beam time, a mixing ratio of 1:2 was chosen as per the earlier mixing ratio tests in chapter 4. Four cathodes of TiO_2:Ag have been measured for around 45 minutes each at mass 44, corresponding most likely to counts of ^{44}Ca. This blank measurement is carried out with commercial TiO_2 powder as a first gauge of what is to be expected.

It should be noted here that the cooler pressure was set to 6 Pa as per the results of the cooler pressure tests and no lasers were used. All currents of ^{48}Ti have been measured after the accelerator in MFC 04 and the counts have been measured in the detector.

To assess the blank level of $^{44}X^{3+}$ and the ratio between $^{44}X^{3+}$ and $^{48}Ti^{3+}$, the counts of the measurement in the detector are read out of the automatic analysis file of the VERA server, as is the measurement time. As explained earlier, the current is also measured within the same run, allowing for a ratio to be calculated.

Figure 6.1 shows the isotope ratio of the first blank level measurement carried out at VERA for TiO^- powder. As is evident, the first turn (the first three data points from each cathode in figure 6.1) shows signs of surface contamination for three of the four depicted cathodes.

The generally lowest level seems to settle around $0.2 \cdot 10^{-12}$ with notable disturbances in turn 3, as can easily be seen by a rise in the isotope ratio by around a factor of ten in some cathodes, possibly due to inclusions in one cathode or due to cross contamination from others.

Other than that, the lowest level of $\approx 10^{-14}$ would, if also true for actual ^{44}Ti samples, be (almost) competitive to established AMS-background levels in literature of around 10^{-14} [10, 7].

The samples analyzed in figure 6.2 have been prepared from Ti-ICP solution, in contrast to all samples before that have been manufactured from commercial TiO_2 powder. In terms of chemistry, just a calcination is performed to turn the Ti in solution to TiO_2. This was not only done to get a more realistic blank level but also to test and adjust the chemistry in chapter 5. Please note that these samples were produced with the same Ti-ICP solution that the samples will be made of later. The overall trend in figure 6.2 shows that the surface contamination was substantial after tests with cathodes that had CaO in it. In this case, the cathode before was a TiO_2:Ag:CaO cathode in 1:2:0.001. As can also be seen, the later turn (before the interruption of the measurements due to a technical defect of the detector window) shows the aforementioned ratio of $\leq 10^{-12}$.

Again, this is without any hypothesized detector separation, which could possibly allow a final ratio of $\approx 5 \cdot 10^{-14}$ or even lower, depending on the exact detector separation and purity of the sample. This number is also taken into account, in accordance with earlier tests, for the creation of the diluted standards, that aim to cover a range from $5 \cdot 10^{-9}$ to $5 \cdot 10^{-12}$ with the latter around

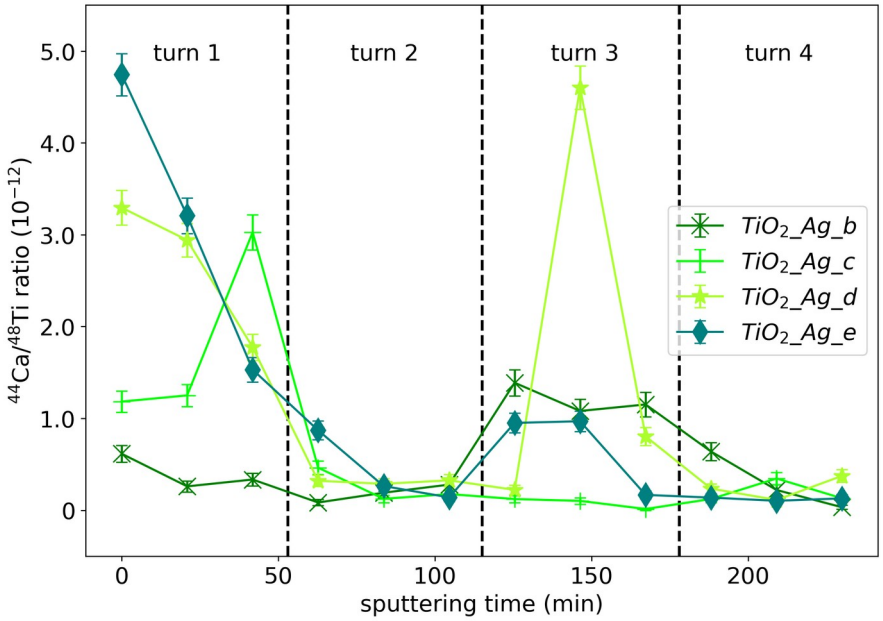

Figure 6.1.: The ratio between the counts of $^{44}Ca^{3+}$ charge and $^{48}Ti^{3+}$. The x-axis shows the measurement time in minutes and the y-axis shows the ratio between $^{44}Ca^{3+}$ and $^{48}Ti^{3+}$. There is a clear decrease after the first three measurements, likely showing some amount of surface contamination. The rough average of the ratio over the full measurement time is $\approx 10^{-12}$, although it should be noted that the lowest continuous level is $\approx 5 \cdot 10^{-13}$.

a factor of 100 above the estimated blank level. The chemistry to prepare these standards can be found in [5].

With that, it can be expected that a measurement of the 510^{-12} standard is subject to only 1% of counts that originate from $^{44}Ca^{3+}$, allowing for small uncertainties compared to the uncertainties from counting statistics.

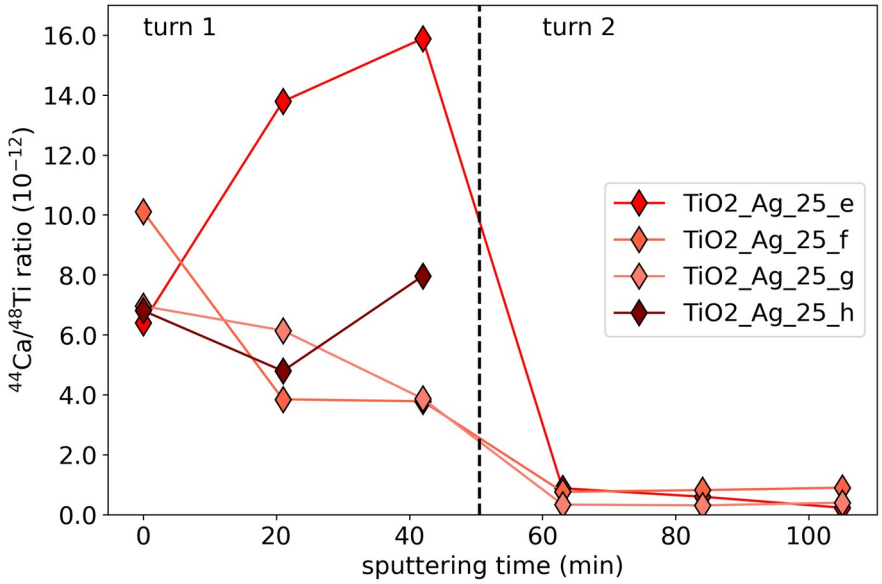

Figure 6.2.: The ratio between the counts at mass 44 with 3+ charge and $^{48}Ti^{3+}$. The x-axis shows the measurement time in minutes and the y-axis shows the ratio between $^{44}Ca^{3+}$ and $^{48}Ti^{3+}$. The black dashed line shows the two different turns. Note that there is a clear difference between the first three measurement points and the next three, likely coming from some surface contamination. The later three also agree with values attained from previous beam times, see figure 6.1, around 10^{-12}. This sets up the reasonably expectable background level of $^{44}Ca^{3+}$ for coming measurements and provides rough guidance for the dilution series steps.

7. The First Measurement of ^{44}Ti at VERA

7.1. Measuring self made ^{44}Ti standards

Preparation

Material overview

As previously stated, the word 'standard' in this work should be seen relative, as the samples used have not been tested in any other way to assure their ratio of $^{44}X^{3+}$ to $^{48}Ti^{3+}$, and can thus not be treated as a primary standard. The ratio is based upon calculations and gamma-measurements at the PSI and assumes a reasonably good chemistry without critical contamination or mistakes. See chapter 5 for details on this process and further explanation.

For the purposes of the measurement, three cathodes for each standard were pressed in a mix of TiO_2 to Ag in the tested optimal of 1:2 (see figure 4.9). All cathodes had 3 mg total material in them and were as usually pressed into copper cathodes and were installed into a copper wheel. In total, 16 cathodes were prepared, three for each of the four standards and three that act as a blank with Ti ICP solution. Not all four standards have been measured, as SMV-Ti-09 (with a ratio of $5{\cdot}10^{-9}$) was expected to saturate the detector and was thus deemed unnecessary.

In addition to the ones seen in table 7.1, some old isobar spiked cathodes have been reused, mainly to asses the ratio of ^{44}Ca in the region of interest over the total amount of ^{44}Ca. The reused cathodes have been from the interrupted beam time in February, so they are TiO_2:Ag:CaO in the ratio 1:2:0.001.

Name	number of cathodes	rough ^{44}Ti activity in cathode (Bq)
SMV-Ti-09	3	16.7
SMV-Ti-10	3	1.49
SMV-Ti-11	3	0.130
SMV-Ti-12	3	0.0149
blank	4	0

Table 7.1.: The kinds of cathodes used for the ^{44}Ti measurements. All cathodes were pressed in a mixture with Ag in a ratio of Ti:Ag in 1:2 in copper cathodes. Information on individual cathodes can be found in table A.4

Please note that the numbers in table 7.1 are estimated from the mass of powder put in, but were themselves not measured. They are to be seen as a rough guide for what to expect.

Measurement procedure

The measurement process itself is no different than for any other sample. By measuring the ion current in MFC 04, the counts in the detector as well as measuring times throughout this process, the ratio between ^{44}Ti and ^{48}Ti can be calculated for each of the standards. The material necessary for such measurements is briefly described in chapter 2 and the ideal measurement techniques have been developed throughout chapter 4.

The pressure in the ion cooler is set to 6 Pa of He as per the earlier results. No OPO laser was available at VERA at the time of measuring, but the ion gas interaction should be enough to measure the fabricated standards. Each turn, the currents and the counts in the detector are measured multiple times, which will be explained in more detail later.

Once a ratio has been calculated per turn, a normalization is carried out with a normalization factor such that the highest of the measured standards fits its nominal value. This normalization is applied over the average of all the cathodes of this type. The same is subsequently carried out with all the other standards as well as the blanks.

Note that the non-normalized measurement results are certainly still valuable, as they will indicate if the prepared samples have been handled reasonably well and if something has gone wrong in chemistry. Fractionation inside VERA can also distort the final measured ratio and also needs to be remembered should the non-normalized results stray too far from their nominal values. If the non-normalized measurement is off by a factor of 100, this could point to an error in some step of the preparation that has gone unnoticed, like some spill or insufficient mixing before cathode pressing. If the difference is only 50%, everything should be fine.

While creating the evaluations of the recorded data, currents are being treated as having no uncertainty, while the uncertainty of the counts are of course assumed to be the square root of themselves, as per Poisson statistics. The uncertainties, both inner and outer, are further calculated using the python module “uncertainties” and is manually checked at random.

To analyze the data after the beam time, several tools are used. VERA comes with it’s own suite of analysis tools and utilities that are used for data acquisition as well as some rudimentary analysis about basic parameters like transmission between the LE side and the HE side.

For more advanced metrics, a python script is used. Uncertainties as well as statistics are also handled within python, so is the visualization. The data from chemistry and weighing has been recorded in Excel tables.

Tuning

To maximize separation in the detector, the terminal voltage was increased to 3 MV for measuring ^{44}Ti, and to 2.8 MV for measuring the ^{48}Ti current in the offset cup in MFC 04.

For the best results, we changed the stripping gas in the pelletron tank to He and the gas in the ion cooler as well. For the best possible suppression, the gas pressure inside the cooler was set to 6 Pa.

Source parameters changed during the beam time, however the cathode voltage CAT remained constant at 4.601 kV. As stated before, after the fourth turn of the beam time, the injection energy was increased by 20 eV in the hopes of dissociating more CaO^- in the cooler than before.

Measurements

In total, five turns of all cathodes except for the second spike and the SMV-Ti-09 (5 $\cdot 10^{-9}$) standards have been measured. The SMV-Ti-09 standards have not been measured at all on purpose, as the The SMV-Ti-10 standards already provided enough counts to be close to the limit of the detector and the higher standard would be at risk to saturate the detector and caused substantial cross contamination in the ion source.

Currents

The currents listed hereafter are all measured in FC04 after the accelerator. Overall the currents can be said to have been relatively stable throughout the whole beam time, with changes only in the 40% range at worst.

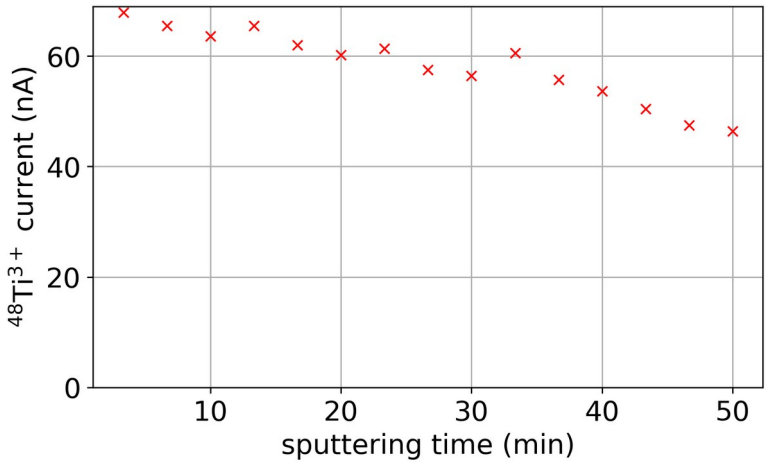

Figure 7.1.: $^{48}Ti^{3+}$ ion current on the y-axis vs. sputter time on the x-axis for a cathode of the SMV-Ti-11 standard. The general trend of current in this cathode is representative for the trend for most cathodes in the ^{44}Ti beam time.

Figure 7.1 shows the current over time from cathode 11, a SMV-Ti-11 standard cathode. While the details can of course vary, the overall trend of all cathodes look similar to this one. The start is close to 65-70 nA in all cases and the current decreases by roughly 40% over the course of the beam time.

There are slight variances in the current, particularly in the last three data points, due to the increase of the cooler injection energy in the last turn. The spikes interestingly reacted the strongest to that change. Other cathodes show increases at some turns, specifically most strongly in the fourth turn, but never exceeding 40%.

Please note that in this figure, three current measurements translate to one turn, even though four current measurements are usually taken during one turn. A rolling average was applied to get the same number of current measurements as counting runs.

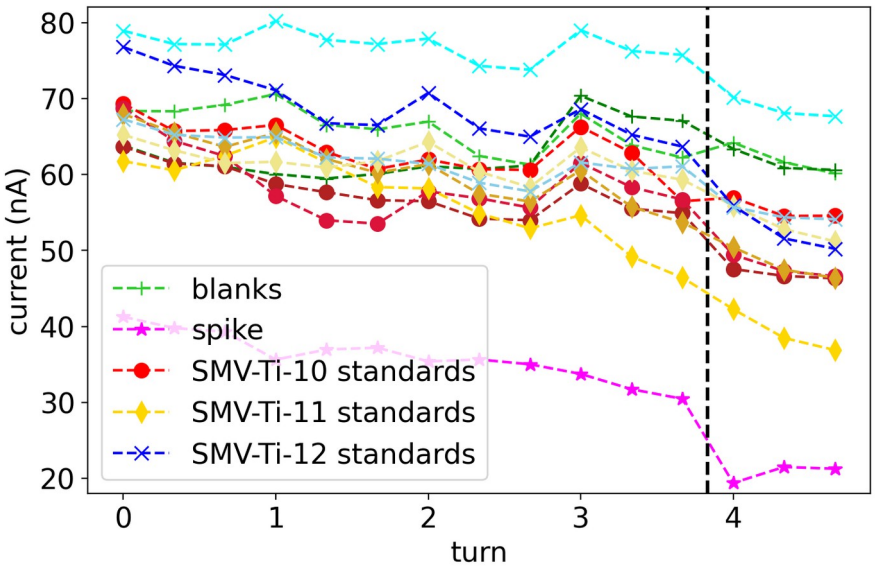

Figure 7.2.: The currents of all cathodes from the measurements of ^{44}Ti samples. The y-axis is the stable $^{48}Ti^{3+}$ current in nA as measured in FC 04 and the x-axis is the sputter time. The last turn is indicated by a black dashed line, after which the injector energy was increased.
The last turn shows a general decrease in currents, with the spike showing the strongest decrease. The total counting time for the spectra of the standards were 50 minutes for the SMV-Ti-10, SMV-Ti-11 and the blanks, around 25 minutes for the SMV-Ti-10 standard and just 12 minutes for the spike cathodes.

Figure 7.2 shows the good stability of the currents throughout the beam time. Please note that the sputter time is per cathode, and not the actual time since the start of the beam time. As can also be seen, the magenta spike shows similar stability until the injection energy into the cooler was increased. It turned out to not make a significant difference when taking into account the lower count rate.

Counts

The counts as recorded by the detector are luckily well separable between ^{44}Ca and ^{44}Ti, more so than expected from previous estimates.

Figure 7.4 shows another detector spectrum. However, the depicted regions of interest are the ones used for evaluation of the collected data. After some testing these conditions prove to be the ones with the best results, see section 7.1 for details. The discarded counts reach relatively far into the Ti region which is due to the somewhat long tailing of Ca counts into the region.

A machine script on the data evaluation server at VERA can automatically apply the cuts to the spectrum and yield a table of counts for each cathode in the beam time. The overall change in counts shows less stability compared to the currents. All in all, a general reduction in counts is observed approximately halving over the duration of the beam time. Notably, during

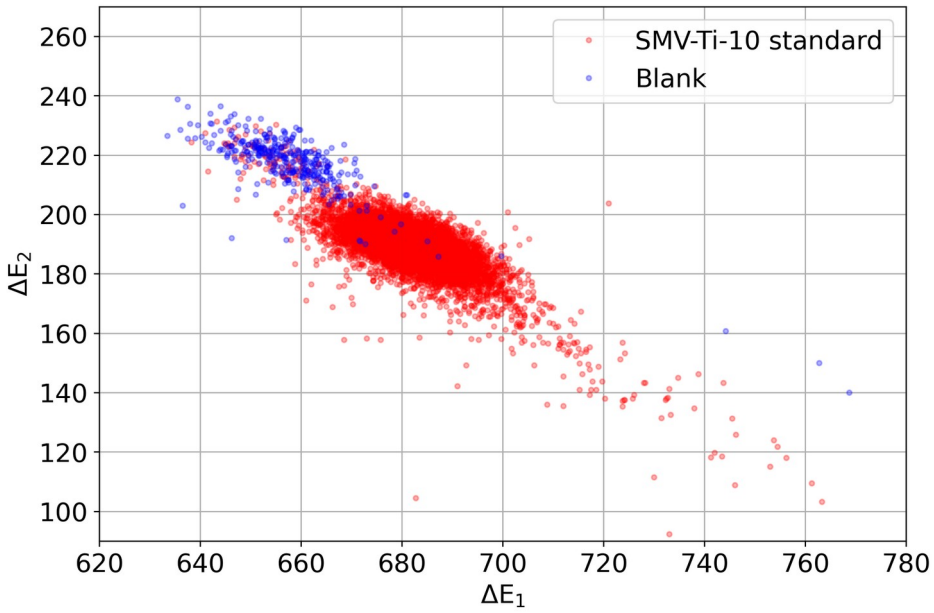

Figure 7.3.: A detector spectrum immediately prior to the start of automatic measurements. The blue counts stem from a blank cathode and are thus mostly ^{44}Ca, while the red counts come from a SMV-Ti-10 cathode containing^{44}Ti. The blue and the red areas barely touch, with the stragglers from the blank contributing the most to the region of interest for the standard once the cut is applied.

the final phase, energy modifications within the cooler induce significant further reductions in certain count rates, such as a decrease in the spike by a factor of five. All count rates decrease significantly in the last turn, but nowhere near the amount as the spike does, typically at most a factor of two.

Ratios

Since the counts decrease stronger than the currents over the course of the beam time, the ratios also diminish with time in the measurement. Typically, about a factor of 40% of the ratio is lost during the beam time if no normalization is applied.

The two measured blanks behave somewhat differently from one another.

Figure 7.5 shows the ratio of the measured blanks of the ^{44}Ti beam time. While the averages of both blanks would agree with previous measurements of commercial TiO_2 within a reasonable range, the disagreement between them raises some questions about sample handling and preparation. However the lower of the two blanks shows levels that come close to the established literature blank level of 10^{-14} [7, 9].

Unfortunately, only two of the four blanks were able to be measured, with one showing signs of contamination far above the other. This is likely due to handling during pressing, but may also be due to the handling during chemistry or from irregularities in the ion source. Alternatively,

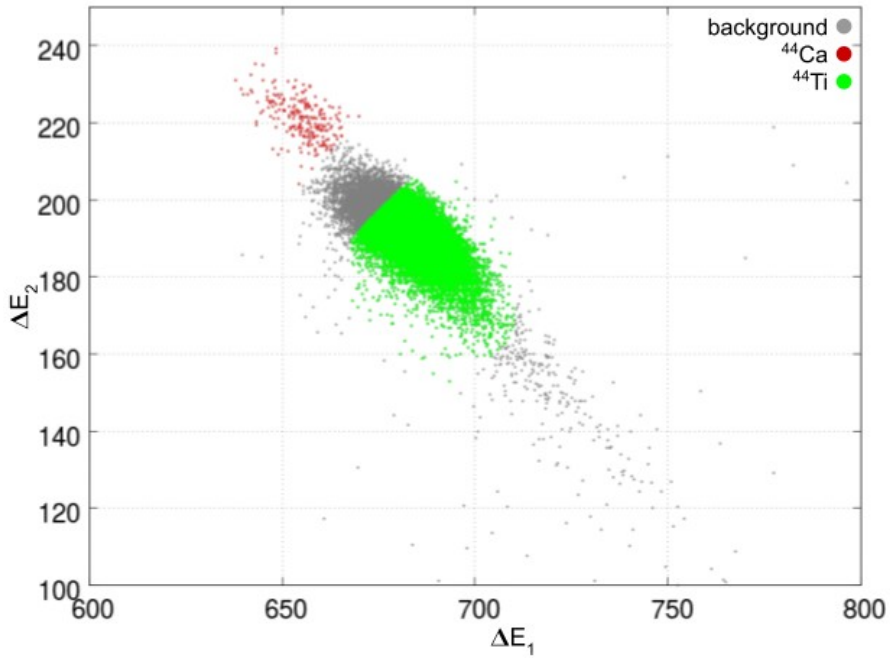

Figure 7.4.: The spectrum of one of the SMV-Ti-11 standards. The x-, and y-axis is the energy loss on the two anodes in the detector. The diverse colors denote different regions of interest with green counted as ^{44}Ti, the lighter red are the counts that are dismissed and the darker red is the ^{44}Ca region. The total counting time for the spectrum of the standard were 100 s.

cross contamination from another cathode to one of the blanks may have taken place. To know how reliable the produced blanks are, a few more should be tested before proceeding to more detailed measurements. Other than that the standards show levels at most 40% lower than their nominal values apart from the last turn.

Figure 7.6 shows the non-normalized ratios ^{44}Ti/^{48}Ti. As can be seen, there are no large deviations from their respective nominal ratios.

Table 7.2 shows the nominal and measured ratios of the ^{44}Ti standards and the blanks. Please note that the measured ratios have of course been averaged for all cathodes of a type.

If the chemistry and handling can be trusted, it is safe to assume that the highest standard should be very close to its nominal value. In the following graphs, a normalization factor per turn is introduced that carries out this specific task.

About every 100th Ca atom hits the Ti region of interest in the blanks as was evaluated from the spike energy loss spectra. With that, the current blanks can be corrected before the normalization to the highest standard. It must be noted here that in the blanks, about 70 to 75% of the counts in the Ti region of interest likely stem from Ca. For the standards, the contribution is almost negligible at roughly 0.5 to 0.01%. Earlier tests with the detector and an estimate of the separation can be found in figure 4.12 and the corresponding text.

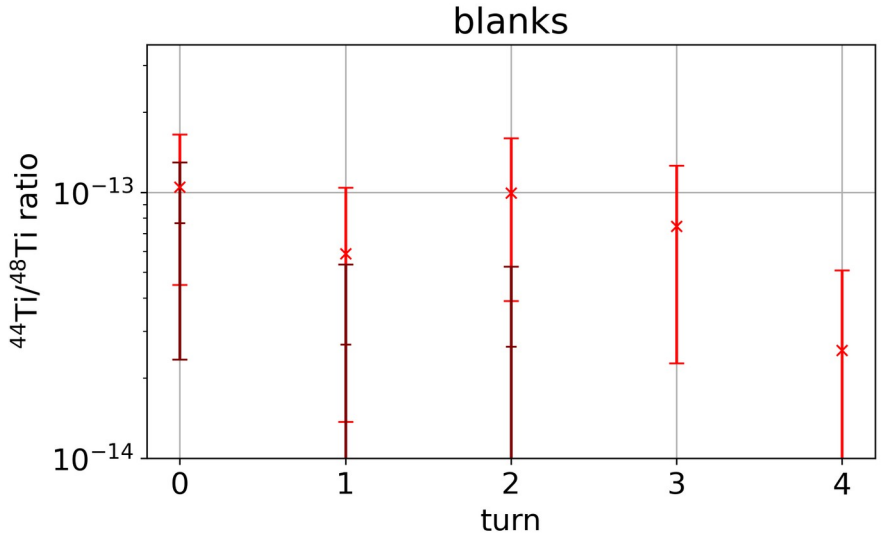

Figure 7.5.: The ratio per turn of both measured blanks. The y-axis shows the ratio of ^{44}Ti to ^{48}Ti and the x-axis shows the turn number starting at 0. The two blanks have a clearly different ratio, apart by usually a factor of two-three. The blanks in this figure have been normalized with SMV-Ti-10. Note that this is without Ca correction.

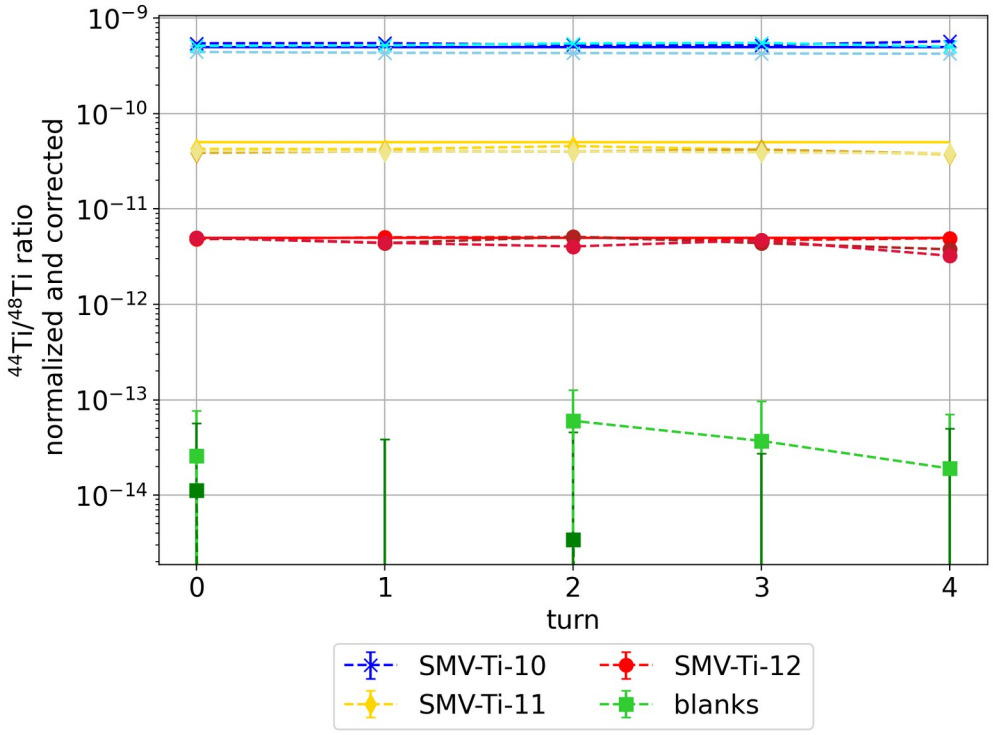

Figure 7.7.: The blanks and the three measured standards per turn and per cathode, normalized. The y-axis shows the ratio of ^{44}Ti to ^{48}Ti and the x-axis shows the turn number starting at 0. The SMV-Ti-10 standards are shown as blue crosses, the yellow diamonds are the SMV-Ti-11 standards and the red dots show the SMV-Ti-12 standards. The blanks are indicated as green squares. As can be seen, the normalized standards fit well with their nominal values by around 20%, baring some deviations in the last turn.

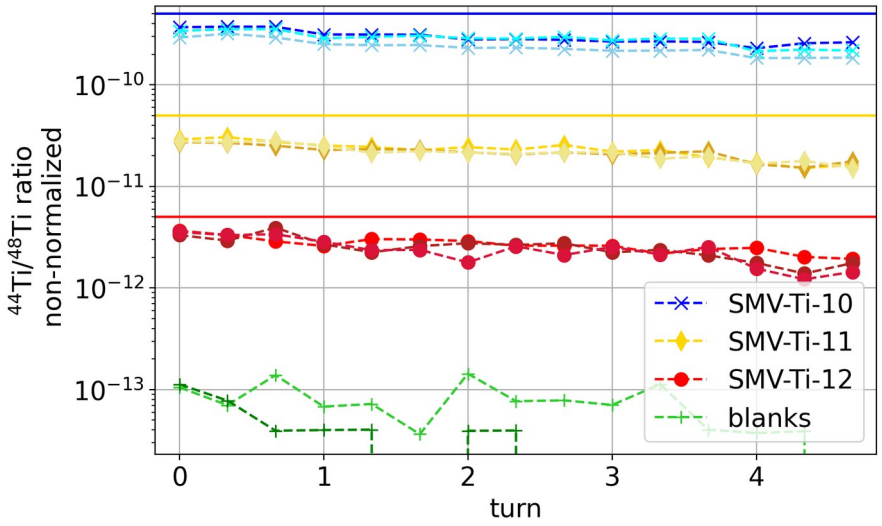

Figure 7.6.: The three measured standards each per cathode. The y-axis shows the ratio of ^{44}Ti to ^{48}Ti and the x-axis shows the sputtering time per cathode in minutes. The blue crosses are the SMV-Ti-10 standards, the yellow diamonds are the SMV-Ti-11 standards and the red dots stand for SMV-Ti-12 standards. The standards each don't stray far from their counterparts and are all similarly below their nominal level by about 15-40%. Note again that his is without any normalization or correction.

The normalized ratios together with the normalized blanks can be seen in Figure 7.7. As is evident, the standards are slightly below their nominal standards, but lie within 20% thereof. The consistency is also to be noted, since all standards seem to be well within roughly a factor of ten from each other. This speaks to the good chemical procedure and handling of the samples during target preparation.

Nominal ratio	Measured ratio ^{44}Ti/^{48}Ti	Normalized ratio
$5{\cdot}10^{-10}$	$(2.74 \pm 0.49) \cdot 10^{-10}$	$(5.00 \pm 0.05) \cdot 10^{-10}$
$5{\cdot}10^{-11}$	$(2.22 \pm 0.39) \cdot 10^{-11}$	$(4.05 \pm 0.14) \cdot 10^{-11}$
$5{\cdot}10^{-12}$	$(2.53 \pm 0.61) \cdot 10^{-12}$	$(4.58 \pm 0.20) \cdot 10^{-12}$
blank	$(4.9 \pm 0.8) \cdot 10^{-14}$	$(2.4 \pm 1.5) \cdot 10^{-14}$

Table 7.3.: The normalized measured ratios together with the respective nominal ratios. Note that the normalized ratio of the blanks also included the isobaric correction carried out with the spikes. Note that for the blanks, the normalized and Ca corrected ratio is lower due to high decreases when carrying out the Ca correction. Note also that the relative uncertainty increases due to the high spread of the two blanks that increases after the Ca correction and normalization.

Table 7.3 shows the ratios when the standards are normalized to SMV-Ti-10. Evidently, the

Nominal ratio	Measured ratio
$5{\cdot}10^{-10}$	$(2.74 \pm 0.49) \cdot 10^{-10}$
$5{\cdot}10^{-11}$	$(2.22 \pm 0.39) \cdot 10^{-11}$
$5{\cdot}10^{-12}$	$(2.53 \pm 0.61) \cdot 10^{-12}$
blank	$(4.9 \pm 0.8) \cdot 10^{-14}$

Table 7.2.: The non normalized measured ratios together with the respective nominal ratios. Note that these measured ratios have been calculated with the severely cut detector spectra that cuts around 45% of the counts that fall inside the Ti region of interest. Please note that this includes the last turn where the injection energy was changed.

normalized ratio are within at worst 20% of their nominal value. The relatively small uncertainties show the good agreement of the standards among themselves.

As noted previously, the blanks are unfortunately not in agreement with each other for the most part. On average, their combined level comes out to $(4.9 \pm 0.8) \cdot 10^{-14}$, which is roughly a factor of 9 above what has been achieved at large AMS facilities [7, 9]. It should be noted here that the average of the blanks is roughly where it was expected from the blank levels established in chapter 6, which was around $7{\cdot}10^{-14}$ assuming the estimated detector separation at the time. However, due to the discrepancy between the blanks, the higher one will be used to assess the sensitivity conservatively. The higher of the two blanks has a mean ratio of $(4.9 \pm 2.5) \cdot 10^{-14}$.

In Figure 7.8, all measured standards per cathode can be seen along their respective nominal values. Evidently, the normalized values fit well to their nominal value averages within 20% and the standards are roughly a factor 10 apart from each other.

Other than that, the hypothetical ratios of the HZDR meteorite samples (see 2.2) can be seen as dashed gray lines show that they are quite a bit lower than the lowest measured standard but either on or above the level of the measured blanks. An estimate of the lowest measurable ratio currently possible at VERA is little higher than the lowest measured sample in literature by about a factor of 12 [7, 20]. The estimate of the current sensitivity at VERA was achieved by taking the mean of the higher blank plus three times its uncertainty which results in $1.24{\cdot}10^{-13}$.

With that said, the current measurements in regards to the standards have shown a reliable and well performing preparation procedure, as can be seen from the consistency within each standard as well as the separation between the standards, which is almost exactly a factor of 10 each time.

Standard material

The relatively small uncertainties of only $\approx$2% throughout the whole chemistry, the ratio of the standards cannot be seriously questioned, baring any mistakes with the original ^{44}Ti sample material. It must be noted here that the 2% come from the counting uncertainty from the PSI, but a comprehensive error budget above that was not provided. This error should thus be used carefully and likely only for internal applications.

Follow up measurements of the seemingly empty eppi in which the ^{44}Ti was transported on the way to Vienna revealed some residual activity still in the eppi, even when washed out. After a γ measurement thereof, it was determined to be $\lesssim$0.9% of the original activity, and thus within the

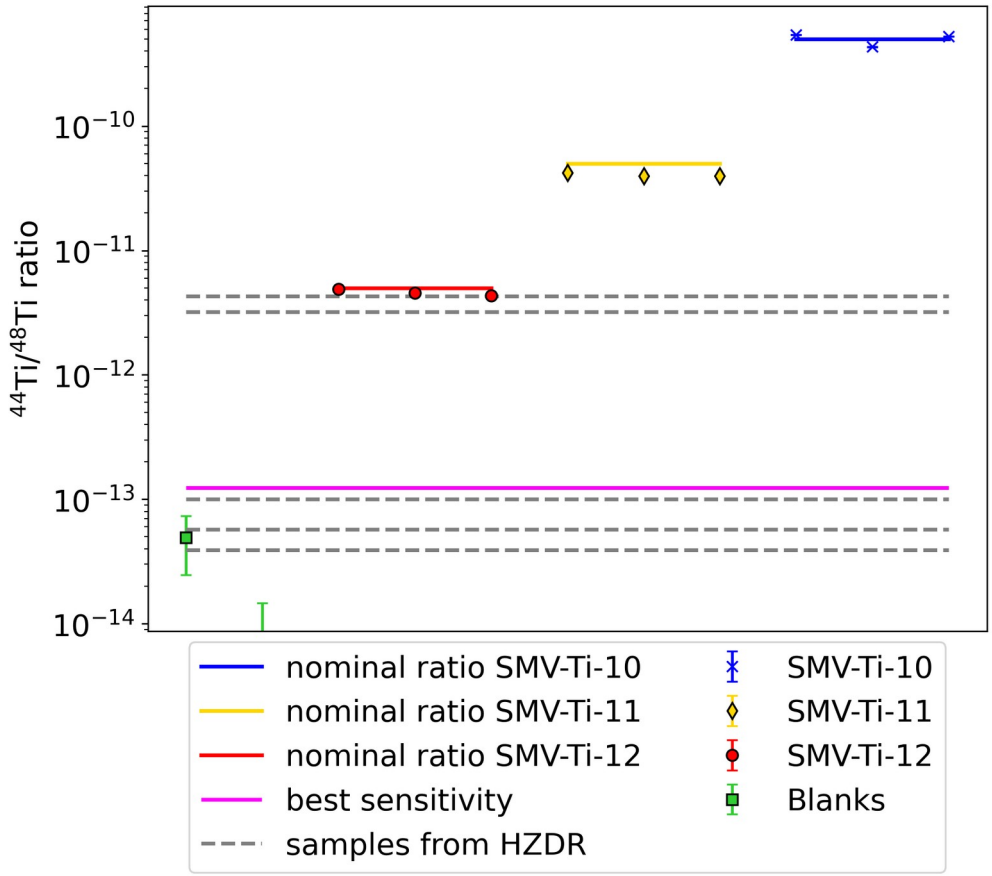

Figure 7.8.: An overview over all results from the ^{44}Ti beam time. The various colored markers depict the various standards and the blanks in the same colors as in previous figures, together with their nominal values as solid lines in the same color. The gray dashed lines signify the hypothetical ratio of samples available at the HZDR. The magenta line shows the estimate of the best case that could be detectable at VERA at roughly $1.24 \cdot 10^{-13}$. Note that this sensitivity was conservatively calculated from the higher of the two blanks.

counting uncertainty of 12 kBq that was given to us as ≈1.8%.

Optimal detector cuts

Figure 7.3 shows how well ^{44}Ti and ^{44}Ca are indeed separated, better than was predicted after a few tests (see Figure 4.13). Even with substantial cuts reaching far into the Ti regions, the regions seen in Figure 7.4 are the most optimal with the best sensitivity & blank levels.

It should be noted that the optimal detector regions were determined via extensive tests, trying eight different cuts into the Ti region. The most important value at which the system cuts the spectra regions is called “COND9” in the VERA system. The COND9 value is one of the

parameters in setting the detector regions, and a higher number means less of the counts are counted as ^{44}Ti and are being discarded.

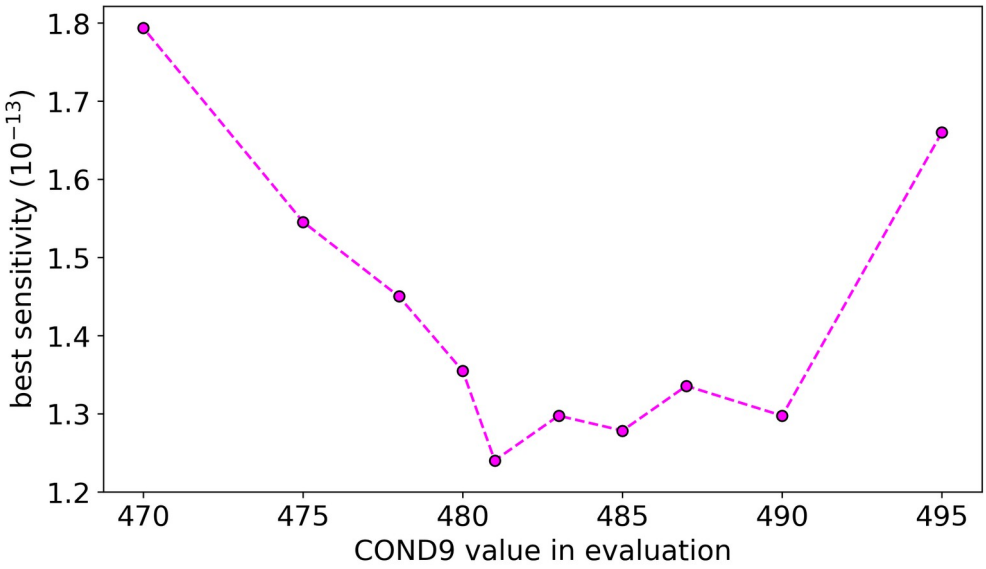

Figure 7.9.: The COND9 value which indicates the depth of the cut into the Ti region, where a higher value means that more counts of Ti are discarded. Note that the best sensitivity is the same as in figure 7.8 and has been evaluated for all the listed COND9 values.

Figure 7.9 shows various results of changing the COND9 value. It can be seen that the ideal value seems to be 481 for this measurement. This means that around 50% of all ^{44}Ti counts will be cut off and discarded due to the influence of ^{44}Ca counts. The overall detector separation is better by roughly a factor of 3-4 than what was expected from the estimations carried out in chapter 4.

If the blanks were more consistent or if more had been created in the first place, a lower sensitivity would likely have been achieved. The lower blank is even slightly negative after normalization, pointing to extremely low amounts of ^{44}Ca in the sample, and the uncertainty from it reaches a little above $1 \cdot 10^{-14}$, which is close to the established values from previous tests at larger AMS facilities [7]. It is not unrealistic that, even without any additional techniques, given better blanks a sensitivity of 10^{-14} may be achieved in the near future.

8. Conclusion & Outlook

Conclusion

The general goal of the project, namely the advancement of the AMS measurement of ^{44}Ti at VERA has been achieved. In particular, the progress of the isobar suppression of ^{44}Ca and the evaluation of the optimal molecule, TiO^-, as well as establishing a blank level and thus isotope ratio of around $1.2 \cdot 10^{-13}$, about a factor of 12 above the lowest sensitivity in literature of $\approx 10^{-14}$, are important milestones for any measurements. This corresponds to roughly $8 \cdot 10^5$ atoms of ^{44}Ti from 1 mg of the typical sample material, TiO_2.

Particularly several samples from various facilities such as the ones available at the Helmholtz Zentrum Dresden Rossendorf would now be possible to be measured at VERA [7, 20].

While the work described so far is the very beginning regarding ^{44}Ti at VERA, a large amount of work still needs to be done before samples may be reliably measured in regards to different Ti carrier material, changes in chemistry and preparation, the behavior in the facility with different mixture ratios beyond what was already measured and much more.

A critical component of this work was the application of a reliable chemical procedure for preparing ^{44}Ti AMS calibration materials. Starting from a 12 kBq ^{44}Ti solution provided by the Paul Scherrer Institute, a dilution series was produced using a stable Ti ICP carrier solutions: Three solutions with ratios of ^{44}Ti/^{48}Ti ranging from $5 \cdot 10^{-10}$ to $5 \cdot 10^{-12}$. Measured ratios agreed with their nominal values within 20% after normalization.

The most significant achievement of this thesis lies in the remarkable suppression of the ^{44}Ca isobar. This was accomplished through a multi-faceted approach within the ILIAMS system. Firstly, the use of a helium gas in the radiofrequency quadrupole ion cooler provided a suppression factor greater than 10^6 by leveraging collisional interactions and chemical reactions that selectively neutralize $^{44}CaO^-$ ions. Secondly, experiments with a temporarily available optical parametric oscillator laser demonstrated the potential for an additional suppression factor of $\approx 10^5$ at photon energies of 0.96 eV (1325 nm), exploiting differences in vertical detachment energies between CaO^- and TiO^-. Finally, an additional separation factor of approximately 150 was achieved in the dual anode ionization chamber by exploiting the differing energy loss profiles of $^{44}Ti^{3+}$ and $^{44}Ca^{3+}$ ions, allowing for software to discriminate against remaining isobaric counts.

The immediate application of this capability is the measurement of irradiated ^{40}Ca targets from previous cross-section studies, which would provide valuable new data to resolve the long-standing discrepancies between observed ^{44}Ti abundances in supernova remnants and theoretical production models. With further refinements, particularly the permanent integration of a high-power infrared laser system, the sensitivity of VERA could be pushed to or below 10^{-14}, potentially surpassing existing literature values and opening new possibilities. The used blanks have unfortunately presented with strongly different ratios, likely as a consequence of handling

and preparation.

Outlook

Given that the standards could all be measured, it may be helpful to put the results in relation to actually existing samples. For the measurements carried out in [19], multiple ^{44}Ti samples have been prepared at the PSI and measured at the HZDR with gamma counting [20]. These targets would have an isotopic ratio between ^{44}Ti and $^{\text{nat.}}$Ti ranging from $2.9{\cdot}10^{-12}$ to $2.6{\cdot}10^{-14}$ based on activity measurements if mixed with 1 mg of stable Ti ICP solution. Given the results of this thesis, the higher targets around 10^{-12} should be measurable without any problems in a few hours at the most. The lower samples are currently out of reach for the sensibility of VERA, but this can be expected to improve with coming tests and the possible addition of an OPO laser.

Due to the focus on oxides after tests with the OPO, no more fluorides have been tested. Several fluoride molecules have been left unchecked for various reasons, such as $TiFO^-$ and $TiFO_2^-$. $TiFO_2^-$ performed better than two of the initially more promising molecules, namely TiF_4^- and TiF_5^- in terms of current over time, baring a rather weak start. As the acquisition of a laser around 1325 nm is not certain, maybe another molecule may show more favorable behavior with the existing lasers at ILIAMS. With this said, other facilities have also opted for TiO_2 as the material of choice for their samples [7, 16].

If the investigation of the lower samples ever turns into a priority, a laser at $\approx$ 1325 nm like the OPO could suppress the isobar by a further $\approx 10^4$ as the investigations herein have shown. This would potentially allow samples with a ratio as low as 10^{-17} of ^{44}X/^{48}Ti to be reliably measured if there was no cross contamination among the cathodes. Currently, no such laser is available permanently at VERA, but has in the past been borrowed.

Assuming around two hours to collect 10 counts of the blanks (at a few 10^{-14}), counting samples significantly lower than that may present a problem with sputtering duration. If anything significantly below 10^{-14} could be achieved as a blank level with a 1325 nm laser, measuring perhaps a sample of 10^{-15} would already require $\approx$20 hours of sputtering for 10 counts, which exceeds the typical time a cathode can be sputtered reasonably.

Technically, many different cathodes filled with the same mixture could be installed and measured for many days to a week that way in order to achieve the necessary counts. But with a lot of cathodes come a lot of contamination possibilities, that at such low rates could have great influence on the overall measurement. Note that no strong cross contamination was found in the tests in this work, but dedicated tests should be carried out. Practically, somewhere around the $5 \cdot 10^{-15}$ mark is the most optimistic limit for measurements at VERA, assuming 5 hours per sample with four samples. Note that this approach would likely require an increase in sample material above $\approx$3 mg for better long time stability, which may be a problem.

^{44}Ti from meteorites is very unlikely to ever be detected at typical AMS facilities. As noted earlier, typical amounts of ^{44}Ti are around 0.1 Bq /kg [6]. At these ranges with the roughly $1.2{\cdot}10^{-13}$ sensitivity currently possible at VERA, close to 20 g of meteorite material would be necessary in order to detect the amounts of ^{44}Ti present. This is without talking about already present ^{48}Ti or any likely contamination with ^{44}Ca. Even if a blank level of $5 \cdot 10^{-15}$ could be achieved at VERA, acquiring 20 g of meteorite material would likely prove difficult, especially

given the destructive nature of the tests and the possibility of needing more material for follow up tests.

It would be interesting to find out what exactly occurs in the cooler to the CaO^- molecules. As pointed out before, it is not known if CaO^- is dissociated or if it is fully detached or broken up. While tests may be difficult due to the ionizer poisoning effect of CaO, it would still be worth testing somewhat extensively. The knowledge may also help with further suppression.

The next measurements should be carried out with tuning cathodes that aren't blanks. For this, commercial Ti can be used, as it's blank level is fully sufficient for tuning with very little cross contamination, if any. Additionally, lower standards below a $^{44}Ti/^{48}Ti$ ratio of $5 \cdot 10^{-13}$ and potentially another even lower one at $5 \cdot 10^{-14}$ should be manufactured, if possible, to reliably test these lower ratios at VERA should it be possible to consistently produce lower blanks.

VERA has recently acquired a titanium sapphire laser that was permanently added to the available lasers at ILIAMS which could hypothetically be used to suppress CaO^-. While TiO^- is already significantly affected at energies $\gtrsim$1.3 eV, the overall suppression of the isobar is very likely higher than the loss in TiO^- and should thus at least be investigated further.

Bibliography

[1] L. S. The, M. D. Leising, J. D. Kurfess, W. N. Johnson, D. H. Hartmann, N. Gehrels, J. E. Grove, and W. R. Purcell. CGRO/OSSE observations of the Cassiopeia A SNR. *Astronomy & Astrophysics*, 120:357–360, 1996.

[2] A. F. Iyudin, R. Diehl, H. Bloemen, W. Hermsen, G. G. Lichti, D. Morris, J. Ryan, V. Schoenfelder, H. Steinle, M. Varendoff, C. de Vries, and C. Winkler. COMPTEL observations of ^{44}Ti gamma-ray line emission form CAS A. *Astronomy & Astrophysics*, 284:L1–L4, April 1994.

[3] I. Ahmad, J. P. Greene, E. F. Moore, S. Ghelberg, A. Ofan, M. Paul, and W. Kutschera. Improved measurement of the ^{44}Ti half-life from a 14-year long study. *Phys. Rev. C*, 74:065803, Dec 2006.

[4] Weinberger, Christoph, Diehl, Roland, Pleintinger, Moritz M. M., Siegert, Thomas, and Greiner, Jochen. ^{44}Ti ejecta in young supernova remnants. *Astronomy & Astrophysics*, 638:A83, 2020.

[5] G Bonino, G Cini Castagnoli, C Taricco, and N Bhandari. Century scale solar variability imprinted in the ^{44}Ti activity in meteorites. *Advances in Space Research*, 17(2):127–130, 1996.

[6] G Bonino, G Cini Castagnoli, N Bhandari, P Della Monica, and C Taricco. Galactic cosmic ray variations in the last two centuries recorded by cosmogenic ^{44}Ti in meteorites. *Advances in Space Research*, 23(3):607–610, 1999. The Transport of Galactic and Anomalous Cosmic Rays in the Heliosphere: Observations, Simulations and Theory.

[7] H. Nassar, M. Paul, I. Ahmad, Y. Ben-Dov, J. Caggiano, S. Ghelberg, S. Goriely, J. P. Greene, M. Hass, A. Heger, A. Heinz, D. J. Henderson, R. V. F. Janssens, C. L. Jiang, Y. Kashiv, B. S. Nara Singh, A. Ofan, R. C. Pardo, T. Pennington, K. E. Rehm, G. Savard, R. Scott, and R. Vondrasek. The ^{40}Ca(α, γ)^{44}Ti reaction in the energy regime of supernova nucleosynthesis. *Physical Review Letters*, 96(4), February 2006.

[8] Tianshu Wang and Adam Burrows. Insights into the Production of ^{44}Ti and Nickel Isotopes in Core-collapse Supernovae. *The Astrophysical Journal*, 974(1):39, 2024.

[9] S.K. Hui, M. Paul, D. Berkovits, E. Boaretto, S. Ghelberg, M. Hass, A. Hershkowitz, and E. Navon. ^{44}Ti atom counting for nuclear astrophysics. *Nuclear Instruments and Methods in Physics Research Section B: Beam Interactions with Materials and Atoms*, 172(1):642–646, 2000. 8th International Conference on Accelerator Mass Spectrometry.

[10] M. Paul, C. Feldstein, I. Ahmad, D. Berkovits, C. Bordeanu, J. Caggiano, S. Ghelberg, J. Goerres, J. Greene, M. Hass, A. Heinz, D. Henderson, S.K. Hui, R.V.F. Janssens, C.L. Jiang, S. Jiang, Y. Nirel, R.C. Pardo, T. Pennington, K.E. Rehm, G. Savard, G. Verri, R. Vondrasek, I. Wiedenhover, and M. Wiescher. Counting ^{44}Ti nuclei from the ^{40}Ca(α, γ)^{44}Ti reaction. *Nuclear Physics A*, 718:239–242, 2003.

[11] M. Martschini, J. Lachner, K. Hain, M. Kern, O. Marchhart, J. Pitters, A. Priller, P. Steier, A. Wiederin, A. Wieser, and R. Golser. 5 Years of Ion-Laser Interaction Mass Spectrometry—Status and Prospects of isobar suppression in AMS by lasers. *Radiocarbon*, 64(3):555–568, 2022.

[12] Walter Kutschera, A. J. Timothy Jull, Michael Paul, and Anton Wallner. Atom counting with accelerator mass spectrometry. *Rev. Mod. Phys.*, 95:035006, 2023.

[13] Multi - Cathode Source of Negative Ions by Cesium Sputtering (MC-SNICS). https://www.pelletron.com/wp-content/uploads/NEC_MC_SNICS_Update_r3.pdf. Accessed: 20th of August 2025.

[14] Martin Martschini, Petra Holzer, Esad Hrnjic, Alfred Priller, Peter Steier, and Robin Golser. Pulsed operation of a snics ion source – ionization efficiency and ion current output. *Nuclear Instruments and Methods in Physics Research Section B: Beam Interactions with Materials and Atoms*, 527:7–11, 2022.

[15] O. Forstner, L. Michlmayr, M. Auer, R. Golser, W. Kutschera, A. Priller, P. Steier, and A. Wallner. Applications of a compact ionization chamber in ams at energies below 1mev/amu. *Nuclear Instruments and Methods in Physics Research Section B: Beam Interactions with Materials and Atoms*, 266(10):2213–2216, 2008. Accelerators in Applied Research and Technology.

[16] M. Paul. Counting rare atoms for nuclear astrophysics. *Acta Physica Polonica Series B*, B40(3):685–694, 2009.

[17] VERA Scheme. https://isotopenphysik.univie.ac.at/fileadmin/user_upload/p_isotopenphysik/images_AMS_at_VERA/VERA_20210916_A0.jpgAccessed: 20th of June 2025.

[18] J. Pitters. Laser photodetachment in a gas-filled RF-quadrupole. 2015.

[19] K. Schmidt, S. Akhmadaliev, M. Anders, D. Bemmerer, Ko. Boretzky, A. Caciolli, D. Degering, M. Dietz, R. Dressler, Z. Elekes, Z. Fülöp, G. Gyürky, R. Hannaske, A. R. Junghans, M. Marta, M. Menzel, F. Munnik, D. Schumann, R. Schwengner, T. Szücs, A. Wagner, D. Yakorev, and K. Zuber. Resonance triplet at E_α = 4.5 MeV in the ^{40}Ca(α, γ)^{44}Ti reaction. *Phys. Rev. C*, 88:025803, Aug 2013.

[20] K. Schmidt. Experimente zur Entstehung von Titan-44 in Supernovae. *HZDR Publications*, 2012.

[21] M. Veicht, I. Kajan, J.-C. David, S. Chen, E. Strub, I. Mihalcea, and D. Schumann. Experiment-based determination of the excitation function for the production of ^{44}Ti in proton-irradiated vanadium samples. *Phys. Rev. C*, 104:014615, Jul 2021.

[22] Core Collapse Supernovae. https://www.physics.rutgers.edu/analyze/wiki/cc_supernovae.html. Accessed: 18th of June 2025.

[23] George C. Jordan, Sanjib S. Gupta, and Bradley S. Meyer. Nuclear reactions important in α-rich freeze-outs. *Physical Review C*, 68(6), December 2003.

[24] D. Robertson, J. Görres, P. Collon, M. Wiescher, and H.-W. Becker.New measurement of the astrophysically important ^{40}ca(α, γ)^{44}ti reaction. *Phys. Rev. C*, 85:045810, Apr 2012.

[25] A. F. Iyudin, E. Müller, and M. Obergaulinger. Titanium hidden in dust. *MNRAS*, 485(3):3288–3295, 2019.

[26] Jacco Vink, J. Martin Laming, Jelle S. Kaastra, Johan A. M. Bleeker, Hans Bloemen, and Uwe Oberlack. Detection of the 67.9 and 78.4 kev Lines Associated with the Radioactive Decay of ^{44}Ti in Cassiopeia A. *The Astrophysical Journal*, 560(1):L79, Sep 2001.

[27] M. Renaud, J. Vink, A. Decourchelle, F. Lebrun, P. R. den Hartog, R. Terrier, C. Couvreur, J. Knödlseder, P. Martin, N. Prantzos, A. M. Bykov, and H. Bloemen. The signature of ^{44}Ti in Cassiopeia A revealed by ibis/isgri on integral. *The Astrophysical Journal*, 647(1):L41, 2006.

[28] C. Vockenhuber, C. O. Ouellet, L. S. The, L. Buchmann, J. Caggiano, A. A. Chen, J. M. D'Auria, B. Davids, L. Fogarty, D. Frekers, A. Hussein, D. A. Hutcheon, W. Kutschera, D. Ottewell, M. Paul, M. M. Pavan, J. Pearson, C. Ruiz, G. Ruprecht, M. Trinczek, and A. Wallner. ^{40}Ca(α, γ)^{44}Ti and the production of ^{44}Ti in supernovae. *Journal of Physics G: Nuclear and Particle Physics*, 35(1), 2008.

[29] L. S. The, M. D. Leising, J. D. Kurfess, W. N. Johnson, D. H. Hartmann, N. Gehrels, J. E. Grove, and W. R. Purcell. CGRO/OSSE observations of the Cassiopeia A SNR. *Astronomy & Astrophysics*, 120:357–360, December 1996.

[30] L. S. The, D. D. Clayton, L. Jin, and B. S. Meyer. Nuclear Reactions Governing the Nucleosynthesis of ^{44}Ti. *The Astrophysical Journal*, 504(1):500–515, September 1998.

[31] R. D. Hoffman, S. A. Sheets, J. T. Harke, N. D. Scielzo, T. Rauscher, E. B. Norman, S. Tumey, T. A. Brown, P. G. Grant, A. M. Hurst, L. Phair, M. A. Stoyer, T. Wooddy, J. L. Fisker, and D. Bleuel. Reaction rate sensitivity of ^{44}Ti production in massive stars and implications of a thick target yield measurement of ^{40}Ca(α, γ)^{44}Ti. *The Astrophysical Journal*, 715(2):1383, May 2010.

[32] N. Liu, C. M. O'D. Alexander, J. Wang, L. R. Nittler, and B. S. Meyer. Radioactive ^{44}Ti Found in 15N-Rich Type AB Presolar SiC Grains. In *86th Annual Meeting of the Meteoritical Society*, volume 86 of *LPI Contributions*, page 6230, August 2023.

[33] Nan Liu, Maria Lugaro, Jan Leitner, Bradley S. Meyer, and Maria Schönbächler. Presolar Grains as Probes of Supernova Nucleosynthesis. *Space Science Review*, 220(8):88, 2024.

[34] Harald A. Enge. Deflecting magnets. In Albert Septier, editor, *Focusing of Charged Particles*, volume 2, pages 203–264. Academic Press, New York, 1967.

[35] X.-L. Zhao, A.E. Litherland, J. Eliades, W.E. Kieser, and Q. Liu. Studies of anions from sputtering i: Survey of mfn-. *Nuclear Instruments and Methods in Physics Research Section B: Beam Interactions with Materials and Atoms*, 268(7):807–811, 2010. Proceedings of the Eleventh International Conference on Accelerator Mass Spectrometry.

[36] Chien-Yuan Hu and Eugene B. Hensley. Electron affinities of the barium chalcogenides. *Journal of Applied Physics*, 40(8):3346–3351, 07 1969.

[37] H. Khalil, F. Le Quéré, C. Léonard, and V. Brites. Theoretical Investigations on CaO Ions: Vibronic States and Photoelectron Spectroscopy. *The Journal of Physical Chemistry A*, 117(44):11254–11260, 2013.

[38] Hongbin Wu and Lai-Sheng Wang. Electronic structure of titanium oxide clusters: TiO_y(y=1-3) and $(TiO_2)_n$(n=1-4). *The Journal of Chemical Physics*, 107(20):8221–8228, 11 1997.

[39] Mary B. Walsh, Rollin A. King, and III Schaefer, Henry F. The structures, electron affinities, and energetic stabilities of TiO_n and TiO_n^-(n=1-3). *The Journal of Chemical Physics*, 110(11):5224–5230, 03 1999.

[40] P. Gaggl. Multiphysics simulation of negative ions in a gas filled RF-quadrupole. Master's thesis, University of Vienna, 2021.

[41] C. A. Prompt and P. M. Quinton. Functions of calcium in sweat secretion. *Nature*, 272(5649):171–172, March 1978.

[42] Matthew S. Fantle, Heather Tollerud, Anton Eisenhauer, and Chris Holmden. The Ca isotopic composition of dust-producing regions: Measurements of surface sediments in the Black Rock Desert, Nevada. *Geochimica et Cosmochimica Acta*, 87:178–193, 2012.

A. Appendix

A.1. Real cathode masses

In the thesis, the cathode masses are given by their planned weight to better communicate the idea behind the measurement. To complement this, the actual masses are given here for each of the tables that have been given in the main parts of the thesis.

A.1.1. Mixing ratio

The real masses for table 4.3 can be found in the following table:

Type	Mixing Ratio	planned sample weight (mg)	real sample weights (mg)
TiO_2_Ag_11	TiO_2:Ag in 1:1	1.67	1.26, 1.50, 1.35
TiO_2_Ag_12	TiO_2:Ag in 1:2	1.67	1.45, 1.80, 1.70
TiO_2_Ag_12	TiO_2:Ag in 1:2	2.50	2.65, 2.51, 2.83
TiO_2_Ag_14	TiO_2:Ag in 1:4	1.67	1.80, 2.09, 1.40

Table A.1.: The real masses for the cathodes used in table 4.3. The real mixture ratios were 1:1.07 for the 1:1 cathodes, 1:2.09 for the 1:2 cathodes and 1:3.86 for the 1:4 cathodes.

A.1.2. OPO experiments

For the first rounds of OPO experiments in October of 2024, the used cathodes were prepared with two mixtures. First there were two cathodes of Ti:Ag in 1:2 and two cathodes of Ti:Ag:Ca in 1:2:0.1 to test for Ca suppression. Note that since it was unclear how long these samples would be sputtered, the goal was to fill them with as much material as possible. Filling a cathode with upwards of 3 mg of the Ti:Ag 1:2 proved somewhat difficult, requiring frequent manipulation with a plastic tool to compact the powder inside the cathode.

Samples

Type	Actual weight (mg)	Ratio
TiO_2:Ag	5.5	1:1.97
	6.7	1:1.97
TiO_2:Ag:CaO	7.1	1:1.87:0.29
	6.8	1:1.87:0.29

Table A.2.: Cathodes used in TiSa2408. Note that the CaO content was too high by about a factor three, but given that the goal were suppression tests, this was accepted.

TiSa experiments

λ (nm)	energy (eV)	Ti^{3+} (nA)
913	1.36	3.81
903	1.37	0.92
893	1.39	0.36
883	1.40	0.18
873	1.42	0.03
853	1.45	0.00

Table A.3.: The current of Ti^{3+} over various photon energies. Note that the laser was always on, so the stable currents with the laser off were not recorded in the same manner as with the OPO in table 4.5.

A.1.3. Standards

Usage of the tables below

Screenshots of the relevant parts of the standard preparation spreadsheet can be found here for all the standard material. The magenta values are the most important values for later steps and for the calculations. Yellow boxes are additional information or inferred quantities from measured ones and are not relevant for the mixing. Orange boxes are measured quantities, in this case almost always weight. In principle, it is calculated how much Ti ICP solution is required to achieve the wanted ratio, after which the whole eppi is weighed. For this, the number of atoms is calculated for the weight and the actual achieved ratio is given in the magenta box on the top left. Note that the given NH_3 drops are not added during that stage, but only after all the mixing has been done, see 5. The chemical yield which acts as a quality control is also listed in magenta in the bottom left. As stated in 5, the final goal was to have around 25-30 mg of TiO_2 in the end.

SMV-Ti-08	not in cathodes later				
44Ti/stable Ti			Ti ICP sol (g)	Total solution (g)	stable Ti conc. (µg/g)
1,032E-08			26,2520	26,3512	9448,63
uncert			uncert	uncert	uncert
2,0E-10			0,0005	0,0005	27,90
uncert (%)			Ti ICP sol (mL)	Total solution (mL)	NH3 drops
1,89			**24,93**	25,025	-
			Mass stable Ti ICP sol (µg)		
			2,49E+05		
			uncert		
			7,4E+02		
	44Ti (atoms)		Ti ICP sol (atoms)	Eppi weight (g)	Eppi+sol weight (g)
	3,23E+13		**3,13E+021**	17,63080	43,9820
	uncert		uncert	uncert	uncert
	6,04E+11		9,25E+018	0,00005	0,0005

Figure A.1.: The first solution step, SMV-Ti-08, that was later not pressed into cathodes.

SMV-Ti-09					
Ratio 44Ti/stable Ti	aliquot SMV-Ti-08 [g]		Ti ICP sol. (g)	Total solution (g)	stable Ti conc. (µg/g)
4,970E-09	**0,979**		**1,049**	2,02720	9471,20
uncert	uncert		uncert	uncert	uncert
9,4E-11	0,00005		0,00005	0,00007	14,49
uncert (%)	Aliquot (ml)		Ti ICP sol. (ml)	Total solution (mL)	NH3 drops
1,88	**0,930**		**0,996**	1,93	53
	Aliquot (%)		Mass stable Ti ICP sol (µg)	--> 5 ml tube	cruc+cap weight (g)
	3,72		9949,82	Ti (mg) in SMV-Ti-09	2,72221
	uncert (based on weight)		uncert		uncert
	0,0002		2,9E+01		0,00005
	44Ti from SMV-Ti-08 (aton	Total stable Ti (mg)	Ti ICP sol (atoms)		Cruc + cap + powder weight (g)
	1,20E+12	19,20003	**1,25E+20**		2,74792
	uncert	uncert	uncert		uncert
	2,25E+10	0,040	3,70E+17		0,00005
	Ti from SMV-Ti-08 (atoms)	Total stable Ti (atoms)		Eppi weight (g)	Eppi+sol weight (g)
	1,16E+20	**2,42E+020**		3,16561	5,19281
Chem. Yield (%)	uncert	uncert		uncert	uncert
89	3,44E+017	5,05E+017		0,00005	0,00005

SMV-Ti-10					
Ratio 44Ti/stable Ti	aliquot SMV-Ti-09 [g]		Ti ICP sol. (g)	Total solution (g)	stable Ti conc. (µg/g)
5,012E-10	**0,20224**		**1,79995**	2,00190	9483,96
uncert	uncert		uncert	uncert	uncert
9,5E-12	0,00005		0,00005	0,00007	25,18
uncert (%)	Aliquot (ml)		Ti ICP sol. (ml)	Total solution (mL)	NH3 drops
1,89	**0,192**		**1,709**	1,90	48
	Aliquot (%)		Mass stable Ti ICP sol (µg)		cruc+cap weight (g)
	10,0		17071,32		2,75811
	uncert (based on weight)		uncert		uncert
	0,0025		5,0E+01		0,00005
	44Ti from SMV-Ti-09	Total stable Ti (mg)	Ti ICP sol (atoms)		Cruc + cap + powder weight (g)
	1,20E+11	18,98595	**2,15E+20**		2,78693
	uncert	uncert	uncert		uncert
	2,24E+09	0,051	6,34E+17		0,00005
	Ti from SMV-Ti-09	Total stable Ti (atoms)		Eppi weight (g)	Eppi+sol weight (g)
	2,41E+19	**2,39E+020**		3,1663	5,16820
Chem. Yield (%)	uncert	uncert		uncert	uncert
101	5,07E+016	6,36E+017		0,00005	0,00005

SMV-Ti-11					
Ratio 44Ti/stable Ti	aliquot SMV-Ti-10 [g]		Ti ICP sol. (g)	Total solution (g)	stable Ti conc. (µg/g)
4,998E-11	**0,19888**		**1,79544**	1,99431	9484,34
uncert	uncert		uncert	uncert	uncert
9,4E-13	0,00005		0,00005	0,00007	25,21
uncert (%)	Aliquot (ml)		Ti ICP sol. (ml)	Total solution (mL)	NH3 drops
1,89	**0,189**		**1,705**	1,89	48
	Aliquot (%)		Mass stable Ti ICP sol (µg)		cruc+cap weight (g)
	9,9		17028,55		2,76554
	uncert (based on weight)		uncert		uncert
	0,0025		5,0E+01		0,00005
	44Ti from SMV-Ti-10	Total stable Ti (mg)	Ti ICP sol (atoms)		Cruc + cap + powder weight (g)
	1,19E+10	18,91472	**2,14E+20**		2,79417
	uncert	uncert	uncert		uncert
	2,23E+08	0,051	6,32E+17		0,00005
	Ti from SMV-Ti-10	Total stable Ti (atoms)		Eppi weight (g)	Eppi+sol weight (g)
	2,37E+19	**2,38E+020**		3,16708	5,16139
Chem. Yield (%)	uncert	uncert		uncert	uncert
101	6,35E+016	6,36E+017		0,00005	0,00005

SMV-Ti-12					
Ratio 44Ti/stable Ti	aliquot SMV-Ti-11 [g]		Ti ICP sol. (g)	Total solution (g)	stable Ti conc. (µg/g)
4,999E-12	**0,19858**		**1,78663**	1,98538	9483,52
uncert	uncert		uncert	uncert	uncert
9,5E-14	0,00005		0,00005	0,00007	25,20
uncert (%)	Aliquot (ml)		Ti ICP sol. (ml)	Total solution (mL)	NH3 drops
1,90	**0,189**		**1,697**	1,89	43
	Aliquot (%)		Mass stable Ti ICP sol (µg)		cruc+cap weight (g)
	10,0		16944,99		2,56297
	uncert (based on weight)		uncert		uncert
	0,0025		5,0E+01		0,00005
	44Ti from SMV-Ti-11	Total stable Ti (mg)	Ti ICP sol (atoms)		Cruc + cap + powder weight (g)
	1,18E+09	18,82839	**2,13E+20**		2,59472
	uncert	uncert	uncert		uncert
	2,22E+07	0,062	6,29E+17		0,00005
	Ti from SMV-Ti-11	Total stable Ti (atoms)		Eppi weight (g)	Eppi+sol weight (g)
	2,37E+19	**2,37E+020**		3,1669	5,15228
Chem. Yield (%)	uncert	uncert		uncert	uncert
101	4,53E+017	7,76E+017		0,00005	0,00005

Name	sample material (mg)	^{44}Ti atoms	Activity ^{44}Ti (Bq)
SMV-Ti-10_a	3.1	$4.04 \cdot 10^{9}$	$1.51 \cdot 10^{0}$
SMV-Ti-10_b	2.4	$3.13 \cdot 10^{9}$	$1.17 \cdot 10^{0}$
SMV-Ti-10_c	2.6	$3.32 \cdot 10^{9}$	$1.24 \cdot 10^{0}$
SMV-Ti-11_a	3.5	$4.00 \cdot 10^{8}$	$1.49 \cdot 10^{-1}$
SMV-Ti-11_b	2.4	$2.80 \cdot 10^{8}$	$1.04 \cdot 10^{-1}$
SMV-Ti-11_c	2.4	$2.77 \cdot 10^{8}$	$1.03 \cdot 10^{-1}$
SMV-Ti-12_a	3.4	$4.17 \cdot 10^{7}$	$1.56 \cdot 10^{-2}$
SMV-Ti-12_b	3.0	$3.71 \cdot 10^{7}$	$1.38 \cdot 10^{-2}$
SMV-Ti-12_c	3.5	$4.35 \cdot 10^{7}$	$1.62 \cdot 10^{-2}$

Table A.4.: Nominal values for the standard dilution series. Note that the standards that were not measured (SMV-Ti-09) are not in the table. Note that the rough target weight was around 3 mg.